

# Investigating bound handling schemes and parameter settings for the interior search algorithm to solve truss problems

Ali R. Kashani<sup>1</sup>  | Raymond Chiong<sup>2</sup>  | Sandeep Dhakal<sup>2</sup> | Amir H. Gandomi<sup>3</sup>

<sup>1</sup>Department of Civil Engineering, University of Memphis, Memphis, Tennessee, USA

<sup>2</sup>School of Electrical Engineering and Computing, The University of Newcastle, Callaghan, New South Wales, Australia

<sup>3</sup>Faculty of Engineering & Information Technology, University of Technology Sydney, Ultimo, New South Wales, Australia

## Correspondence

Raymond Chiong, School of Electrical Engineering and Computing, The University of Newcastle, Callaghan, NSW 2308, Australia.

Email:

raymond.chiong@newcastle.edu.au

## Abstract

The interior search algorithm (ISA) is an optimization algorithm inspired by esthetic techniques used for interior design and decoration. The algorithm has only one parameter, controlled by  $\theta$ , and uses an evolutionary boundary constraint handling (BCH) strategy to keep itself within an admissible solution space while approaching the optimum. We apply the ISA to find optimal weight design of truss structures with frequency constraints. Sensitivity of the ISA's performance to the  $\theta$  parameter and the BCH strategy is investigated by considering different values of  $\theta$  and BCH techniques. This is the first study in the literature on the sensitivity of truss optimization problems to various BCH approaches. Moreover, we also study the impact of different BCH methods on diversification and intensification. Through extensive numerical simulations, we identified the best BCH methods that provide consistently better results for all truss problems studied, and obtained a range of  $\theta$  that maximizes the ISA's performance for all problem classes studied. However, results also recommend further fine-tuning of parameter settings for specific case studies to obtain the best results.

## KEYWORDS

boundary constraint handling, interior search algorithm, metaheuristic algorithms, truss structures

## 1 | INTRODUCTION

Finding the optimal design of structures, and truss structures in particular, is important yet challenging. It is time-consuming and requires much trial and error to find a credible solution that minimizes the weight of truss structures while satisfying bounds on design variables, stress, and deflection constraints. Structural optimization has therefore been the subject of many studies. Over the past decades, many researchers have utilized a variety of algorithms to solve similar problems, such as retaining wall optimization,<sup>1-3</sup> shallow footing optimization,<sup>4,5</sup> optimal design of concrete frames,<sup>6</sup> and truss structure optimization.<sup>7</sup>

The quality of the optimized design is directly related to (1) having a robust algorithm and (2) proper handling of constraints. Much effort has been devoted to the first, where various optimization methods for solving the problems faster

This is an open access article under the terms of the Creative Commons Attribution-NonCommercial-NoDerivs License, which permits use and distribution in any medium, provided the original work is properly cited, the use is non-commercial and no modifications or adaptations are made.

© 2021 The Authors. *Engineering Reports* published by John Wiley & Sons Ltd.

or addressing large-scale cases have been developed (Gandomi et al,<sup>8-10</sup> Sahab et al,<sup>11</sup> Yang et al,<sup>12</sup> and Kashani et al<sup>13</sup>). Most of the complex real-world engineering problems, however, are concerned with a search space confined by equality, inequality, and boundary constraints. The performance of an optimization algorithm thus depends highly on how these constraints are handled. Clearly, boundary constraint handling (BCH) is an important step that leads the algorithm to an appropriate outcome (e.g., see Gandomi et al,<sup>14,15</sup> Gandomi and Kashani,<sup>16</sup> Trivedi,<sup>17</sup> Helwig et al,<sup>18</sup> Padhye et al<sup>19</sup>). Nevertheless, prior work considering the impact of BCH in this context is scarce.

In this paper, we apply an art-inspired optimization algorithm developed by Gandomi,<sup>20</sup> known as the interior search algorithm (ISA), to find optimal weight design of truss structures with frequency constraints. The ISA mimics esthetic techniques utilized for interior design and decoration in its attempt to find an optimal solution. Similar to other meta-heuristic algorithms,<sup>21,22</sup> it explores the solution space through two main phases: exploration and exploitation. Previous studies based on different mathematical and engineering benchmark problems have demonstrated that the ISA is able to outperform many other well-known optimization algorithms.<sup>20</sup>

One of the most important features of the ISA is that it can be set by adjusting only one parameter, controlled by  $\theta$ . We investigate how  $\theta$  can influence optimization results, and also evaluate the efficiency of the most common deterministic and probabilistic BCH schemes. Comprehensive numerical simulations reveal that both the parameter settings and BCH schemes play a critical role in determining the algorithm's performance, and that different parameter values and BCH schemes yield different optimization results.

The rest of this paper is organized as follows. In Section 2, the optimum design of truss structures is explained by introducing an objective function that takes natural frequency limitations into account. In Section 3, the ISA and its main parameter are described. Following this, 13 different BCH approaches are presented in Section 4. Numerical results obtained for two 2-D and two 3-D truss benchmark cases are discussed in Section 5, and we dedicate the final section to discuss the results and draw conclusions.

## 2 | OPTIMUM DESIGN OF TRUSS STRUCTURES

Size optimization of truss structures is defined as finding the minimum value for the total weight of the structures, which satisfies natural frequency related constraints.<sup>23</sup> Optimum design of the structures is expressed by the following objective function:

$$\text{Minimize } W(A) = \sum_{i=1}^{NM} \gamma_i A_i l_i \quad (1)$$

where  $W(A)$  is the weight of the structure,  $NM$  is the number of structural elements, and  $\gamma_i$ ,  $l_i$ , and  $A_i$  are the material density, length, and cross-sectional area of the  $i$ th element, respectively.

It is necessary to satisfy inequality constraints in order to incorporate structural requirements that restrict the final design, as follows:

$$\begin{cases} f_g \leq f_g^*, & \text{for some natural frequencies } g \\ f_h \geq f_h^*, & \text{for some natural frequencies } h \end{cases} \quad (2)$$

where  $f_g$  and  $f_h$  are the  $g$ th and  $h$ th natural frequencies of the structure, respectively; and  $f_g^*$  and  $f_h^*$  are the upper and lower bounds on the natural frequencies of the structure, respectively.

## 3 | METHODS

### 3.1 | Interior search algorithm

The art-inspired ISA, developed by Gandomi,<sup>20</sup> is one of the most recent optimization algorithms. It mimics the esthetics or beauty techniques used for interior design and decoration of a specific space. This algorithm searches the solution space by taking advantage of the following two main features of interior design:

1. composition design to provide exploration
2. mirror work to provide exploitation.

The first feature is an interior design process, and proposes a proper composition of elements to create an attractive environment. The second feature is based on the mathematical model of a kind of fine art named “mirror work”. In mirror work, designers innovatively employ a certain number of mirrors to create an attractive decoration. Gandomi<sup>20</sup> modeled this rule by placing a mirror near the global best to find better views. To that end, the solutions (elements), except the best solution, are divided into two groups: the *composition group* and the *mirror group*. The positions of elements in the composition group are altered to produce a beautiful design that addresses diversification. Then, elements in the mirror group are placed between elements in the composition group and the best-selected solution, in order to achieve an enhanced solution that will eventually provide intensification.

Detailed steps of the ISA are as follows:

1. Initialize the first generation within upper bound  $UB$  and lower bound  $LB$ , randomly.
2. Determine the best solution for the  $j$ th iteration,  $x_{gb}^j$ .
3. Divide the remaining elements into two groups, composition and mirror, randomly by a probability of  $\alpha$ . For each element, if  $r_1 < \alpha$ , it is assigned to the mirror group; otherwise it is assigned to the composition group.  $r_1$  is a random value between 0 and 1.
4. Change the arrangement of elements in the composition group using the following equation:

$$x_i^j = LB^j + (UB^j - LB^j) \times r_2 \quad (3)$$

where  $x_i^j$  represents the  $i$ th element in the  $j$ th iteration, and  $LB^j$  and  $UB^j$  denote lower and upper bounds of the composition group in the  $j$ th iteration, respectively.  $r_2$  is a random number between 0 and 1.

5. Place a mirror between each element in the composition group and the best solution, based on the following equation:

$$x_{m,i}^j = r_3 x_i^{j-1} + (1 - r_3) \times x_{gb}^j \quad (4)$$

where  $r_3$  is a random number between 0 and 1, and  $x_{gb}^j$  is the global best solution at iteration  $j$ . Thus, the resulting solution will emerge at a distance of  $x_i^j$  with respect to the mirror's location, where

$$x_i^j = 2x_{m,i}^j - x_i^{j-1} \quad (5)$$

6. Slightly alter the position of the best solution using Equation (6) to further improve its position to the extent possible:

$$x_{gb}^j = x_{gb}^{j-1} + r_n \times \lambda \quad (6)$$

where  $r_n$  is a vector of normally distributed random numbers with its size equal to  $x$ , and  $\lambda$  is a scale factor set to  $0.01 \times (UB-LB)$ .

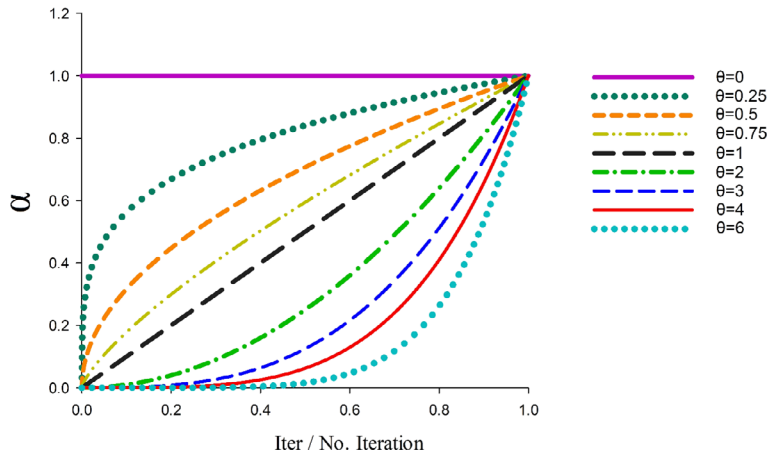
7. After evaluation of the objective function for the new location of both elements and images, update every location using the following equation as a minimization problem:

$$x_i^j = \begin{cases} x_i^j & f(x_i^j) < f(x_i^{j-1}) \\ x_i^{j-1} & else \end{cases} \quad (7)$$

8. Iterate the above mentioned steps until the termination criterion is met.

### 3.2 | Tuning the ISA parameter

In addition to the population size and the number of iterations, the ISA has only one parameter called  $\alpha$ . This parameter is used to assign solutions to either the composition or the mirror group. An initial study by Gandomi<sup>20</sup> showed that its value

FIGURE 1 Effects of  $\alpha$  during iterations

should be approximately 0.25 for unconstrained optimization problems. However, studies on constrained engineering problems<sup>23</sup> demonstrated that it is better to change  $\alpha$  during the iterations. In these studies,  $\alpha$  was linearly increased during the iterations; thus, the search emphasizes exploration by using composition optimization in the early stages and it gradually switches to mirror search to encourage exploitation in the final iterations.<sup>24</sup> In the current study, different nonlinear strategies have been used to adjust the  $\alpha$  parameter. For this purpose, the following formulation is used:

$$\alpha = \left( \frac{Iter}{Max\ No.Iter} \right)^\theta \quad (8)$$

where  $Iter$  is the current iteration number,  $Max\ No.Iter$  is the maximum number of iterations, and  $\theta$  is the parameter to control the nonlinearity. As  $\alpha$  is related to  $\theta$ , different values have been considered for  $\theta$  such as 0, 0.25, 0.5, 0.75, 1, 2, 3, 4, and 6 to take various nonlinearities into account during the iterations. The nonlinear behavior of  $\alpha$  during iterations is visualized in Figure 1.

### 3.3 | Constraint handling

In most constraint optimization problems, the feasible solution space is explored to find the best design as follows:

$$\begin{aligned} & \text{Minimize } f(\vec{x}) \\ & \text{subject to } \begin{cases} g_j(\vec{x}) \geq 0 & j = 1, \dots, J \\ h_k(\vec{x}) = 0 & k = 1, \dots, K \\ x_i^l \leq x_i \leq x_i^u & i = 1, \dots, n \end{cases} \end{aligned} \quad (9)$$

where  $g_j(\vec{x})$  is the inequality constraint,  $h_k(\vec{x})$  is the equality constraint, and  $[x_i^l, x_i^u]$  define the boundary constraints. Optimization algorithms were originally designed for solving unconstrained problems. However, there are several methods to convert a constrained optimization problem into an unconstrained one, such as penalty functions, separation of objectives and constraints, maintaining feasible solutions, and hybrid approaches.<sup>24</sup>

The ISA uses a competitive procedure in combination with the following rules based on Becerra et al<sup>25</sup>:

1. Between two feasible solutions, the better solution is preferred.
2. A feasible solution is preferred to an infeasible one.
3. Between two infeasible solutions, the solution with a lower constraint violation value is preferred.

Here, the constraint violation is calculated using the following equation:

$$violation(x) = \sum_{i=1}^N \frac{g_i(x)}{g_{max\ i}} \quad (10)$$

where  $N$  is the number of constraints,  $g_i$  is the  $i$ th constraint, and  $g_{maxi}$  is the largest violation of the constraint  $g_i(x)$  found so far.

By the second and third rules, the algorithm will explore feasible solutions gradually, and due to the first rule, the algorithm will find an optimized feasible solution.

Originally, this algorithm uses evolutionary BCH formulated as follows:

$$f(z_i \rightarrow x_i) = \begin{cases} r_1 \times x_i^l + (1 - \alpha)x_i^b & \text{if } z_i < x_i^l \\ r_2 \times x_i^u + (1 - \beta)x_i^b & \text{if } z_i > x_i^u \end{cases} \quad (11)$$

where  $r_1$  and  $r_2$  are random numbers between 0 and 1. For  $i$ th design variable,  $x_i^b$  is the related component of the global best solution and  $z_i$  is related to the violated particle (i.e., infeasible solution).

### 3.4 | Population diversity

In order to evaluate the impact of each BCH method on the diversification and intensification of the ISA, population diversity based on  $L_1$  norm is utilized in this study.<sup>26</sup> To this end the following equations are used:

$$\bar{x} = \frac{1}{m} \sum_{i=1}^m x_{ij} \quad (12)$$

$$D_j^p = \frac{1}{m} \sum_{i=1}^m |x_{ij} - \bar{x}_j| \quad (13)$$

$$D_p = \frac{1}{n} \sum_{j=1}^n D_j^p \quad (14)$$

where each particle is represented as  $x_{ij}$ ,  $i$  represents the  $i$ th particle,  $i = 1, \dots, m$ , and  $j$  is the  $j$ th dimension,  $j = 1, \dots, n$ .  $\bar{x} = [\bar{x}_1, \dots, \bar{x}_j, \dots, \bar{x}_n]$ , and  $\bar{x}$  represents the mean of the particles' current positions on each dimension.  $D_p = [D_1^p, \dots, D_j^p, \dots, D_n^p]$  measures the diversity of the particles' positions based on  $L_1$  norm for each dimension and  $D_p$  measures the population diversity of the entire swarm.

## 4 | DIFFERENT BOUND CONSTRAINT HANDLING APPROACHES

For every objective function, design variables vary within a permissible domain defined by bound constraints. Several strategies have been developed in the literature to guide the search into the valid solution domain. In this section, we review various methods for boundary handling.

### 4.1 | Absorbing scheme

This method replaces every invalid value of design variables that violate side constraints with the nearest bound values as follows<sup>27</sup>:

$$z_i \rightarrow x_i = \begin{cases} x_i^l & \text{if } z_i < x_i^l \\ x_i^u & \text{if } z_i > x_i^u \end{cases} \quad (15)$$

### 4.2 | Random method

In this method, invalid values of design variables that violate side constraints are updated randomly, as follows, in order to bring the solution back to the valid search space<sup>27</sup>:

$$z_i \rightarrow x_i = x_i^l + r \times (x_i^u - x_i^l) \quad \text{if } z_i < x_i^l \text{ or } z_i > x_i^u \quad (16)$$

### 4.3 | Random-all approach

This approach does not adjust design variables individually; instead, every infeasible candidate is replaced by a new randomly produced solution within the solution space<sup>28</sup>:

$$z \rightarrow x = x^l + r \times (x^u - x^l) \quad \text{if } z_i < x_i^l \text{ or } z_i > x_i^u \quad (17)$$

### 4.4 | Conservation scheme

In this method, each design variable violating its side constraints is left unchanged.<sup>28</sup>

### 4.5 | Infinity scheme

This approach is similar to the conservation method, but leaves the entire solution vector unchanged if it contains an invalid solution.<sup>29</sup>

### 4.6 | Periodic method

This method uses a modulo operation to replicate an infinite number of solution spaces to bring the trial vector into the valid search domain as follows<sup>30</sup>:

$$z_i \rightarrow x_i = x_i^l + (z_i \text{MOD}(x_i^u - x_i^l)) \quad \text{if } z_i < x_i^l \text{ or } z_i > x_i^u \quad (18)$$

### 4.7 | Mirror scheme

The mirror scheme avoids violating the upper and lower limits of variables. When any variable exceeds its upper or lower bound, it is replaced with a mirror image related to the boundary. In this approach, the main effort is to relieve periodic method faults and reach a more sophisticated scheme, as follows<sup>18</sup>:

$$z_i \rightarrow x_i : x_i^l + z_i \text{MOD}(2 \cdot x_i^u - x_i^l) \quad (19)$$

$$f(z_i \rightarrow x_i) = \begin{cases} f(x) & \text{if } x_i^l \leq z_i \leq x_i^u \\ f(2 \cdot x_{max} - x) & \text{if } x_i^u \leq z_i \leq 2x_i^u \end{cases} \quad (20)$$

where  $z_i$  is the current violated position of the  $i$ th element and  $x_i$  is the updated variable. Based on this method, the objective value would be evaluated using Equation (20).

### 4.8 | Evolutionary bound constraint handling (EBCH)

This approach can be used on any optimization algorithm and is capable of effectively improving the algorithm's performance. See Section 3.3 for details.

### 4.9 | Exponentially confined (Exp-C) approach

The exponentially confined method brings an invalid solution back into the search space between its previous solution and violated boundary.<sup>31</sup> This probabilistic method follows a distribution that guides the new solution toward the violated bounds using the following equation:

$$z_i \rightarrow x_i : x_i = \begin{cases} z_i^p - \ln(1 + r(\exp(x_i^p - x_i^l) - 1)) & \text{if } z_i < x_i^l \\ z_i^p + \ln(1 + r(\exp(x_i^u - x_i^p) - 1)) & \text{if } z_i \geq x_i^u \end{cases} \quad (21)$$

where  $z_i^p$  is the current position of the  $i$ th particle.

#### 4.10 | Exponential spread (Exp-S) approach

This method is a variation of the Exp-C scheme that sets probability distribution along the feasible boundaries, but is biased toward the violated bound.<sup>31</sup> Its computation procedure is defined by the following equation:

$$z_i \rightarrow x_i : x_i = \begin{cases} x_i^u - \ln(1 + r(\exp(x_i^u - x_i^l) - 1)) & \text{if } z_i < x_i^l \\ x_i^l + \ln(1 + r(\exp(x_i^u - x_i^l) - 1)) & \text{if } z_i \geq x_i^u \end{cases} \quad (22)$$

#### 4.11 | Inverse parabolic (IP) constraint-handling methods

In this method, the amount of violation of the boundaries is also taken into account.<sup>19</sup> To be more precise, the probability distribution function may depend on the distance between invalid solutions and the boundaries. Therefore, the probability would be higher for shorter distances to the boundaries, while being far from the boundaries follows a more uniform distribution with lower probability. The following equation proposes a simplified procedure for this approach:

$$\bar{y} = \bar{x}^c + \hat{d}(\bar{x}^p - \bar{x}^c) \quad (23)$$

where  $\bar{x}^c$  and  $\bar{x}^p$  are the invalid and parent solutions, respectively.  $\hat{d}$  is calculated by the following equation:

$$\hat{d} = d_v + \xi d_r \tan\left(r \tan^{-1} \frac{d_r - d_v}{\alpha d_v}\right) \quad (24)$$

where  $d_v$  is the Euclidian distance between the violated particle and the violated boundary,  $d_r$  is the distance between the violated particle and the reference point, and  $\xi$  is a pre-defined parameter. In the original study<sup>19</sup>, this value was proposed to be  $\xi \approx 1.2$ .

By defining  $d_r$ , two variations of this method are proposed: (1) an inverse parabolic confined (IP-C) method that defines a probabilistic distribution function in the space between the parent solution and the violated boundary; and (2) an inverse parabolic spread (IP-S) method that defines a distribution function between the upper and lower bounds.

#### 4.12 | Probabilistic evolutionary bound constraint handling (PEBCH)

PEBCH is a new variation of the IP method, proposed by Gandomi and Kashani,<sup>32</sup> which considers a probability distribution function in the space between the best-found solution and the violated boundary.

#### 4.13 | Flyback bound constraint handling

A Flyback mechanism was proposed by He et al<sup>33</sup> for handling the bound of a particle swarm optimization algorithm. Based on this approach, every violated design variable would be reset to the previous position. In this study, the position of the best solution was also utilized for modifying improper solutions. Thus, every violated design variable is pushed to the position of the best solution. This method is referred to as Flyback-best in our numerical simulations.

In Equations (16), (17), (21), (22), and (24), the parameter  $r$  represents a random number.



## 5 | TEST PROBLEMS AND OPTIMIZATION RESULTS

The performance of the ISA combined with different BCH schemes was analyzed using four benchmark cases with multiple frequency constraints. The algorithm was coded in MATLAB. Because of its stochastic behavior, each experiment was repeated for 50 runs; and the final results were interpreted using the best, worst, and mean optimized weights along with the standard deviation (SD). To adjust the ISA's main parameter, a parametric study was done for  $\theta$  values in the range of 0, 0.25, 0.5, 0.75, 1, 2, 4, and 6. The population size was 50 for all the case studies.

### 5.1 | Interpretation of the results based on best, mean, and standard deviation

In this section, numerical results are presented based on the best, mean, and SD results to assess the performance of the ISA. In the first step, the best results are normalized between the best and the worst solutions found. Obviously, the lowest normalized value is representative of the best method. In each subsection, a number of tables are provided to visualize differences between the applied BCH methods. Regarding the tables, it should be noted that, for each case study, a full comparison between the mean values is initially illustrated; then, the best algorithms whose performance is close to the normalized best values are selected for a more detailed comparison. Moreover, figurative contrasts of the BCH methods for the best  $\theta$  value are depicted using Mean and SD values.  $\theta = 1$  is considered as a benchmark since it provided the best performance in most cases. In case of inconsistency, results obtained for the best value of  $\theta$  are compared with those obtained for  $\theta = 1$ . Convergence curves are presented based on the most successful solution considering the minimum best and mean values found. Population diversity variations in each iteration are evaluated and presented to analyze the effects of different BCH methods on diversification and intensification.

#### 5.1.1 | Planar 10-bar truss

The first test problem solved to analyze the performance of the ISA considers a simple 10-bar truss structure. This problem has been the subject of many studies as a benchmark structural design problem with multiple frequency constraints.<sup>34-36</sup> This problem has been solved by considering various values of modulus of elasticity, material density, and added mass.<sup>37-39</sup> Material properties, constraints, and side constraints used in this study are presented in Table 1. The configuration of the truss is shown in Figure 2; a non-structural mass equal to 454 kg is applied to the four highlighted free nodes in the figure.

The average values of optimized weight obtained over 50 runs are summarized in Table 2, and the normalized best and mean values are presented in Tables 3 and 4, respectively, to make the comprehension of the obtained results more sensible. From Table 3, we can see that the lowest cumulative normalized value based on the best-found solutions is 0.595 for the Flyback-best method. Similarly, Table 3 shows that the Aggregate  $\theta$  value is minimum at  $\theta = 4$ . However, the minimum aggregate values based on the mean solutions suggest the use of the Flyback BCH method and  $\theta = 3$  (Table 4). Table 3 shows that the lowest cost value was recorded by the Mirror BCH method and  $\theta = 3$ . The lowest mean value was, however, obtained by the Flyback-best method with  $\theta = 3$ . Therefore, after a comparison of the normalized mean values, we filtered out the following BCH methods with higher cumulative normalized values: Random, Random-all, Infinity,

Property	Value (unit)
Modulus of elasticity ( $E$ )	$6.89 \times 10^{10}$ (N/m <sup>2</sup> )
Material density ( $\rho$ )	2770 (kg/m <sup>3</sup> )
Design variable lower bound	$0.645 \times 10^{-4}$ (m <sup>2</sup> )
Design variable upper bound	$50 \times 10^{-4}$ (m <sup>2</sup> )
Frequency constraints	$f_1 \geq 7, f_2 \geq 15, f_3 \geq 20$ (Hz)

TABLE 1 Design parameters of planar 10-bar truss



**FIGURE 2** Schematic of the planar 10-bar truss structure

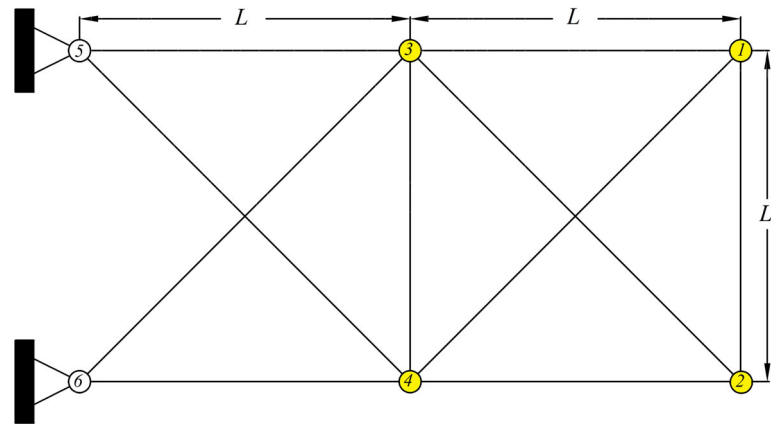


**TABLE 2** Mean values of the optimized weight obtained for the 10-bar truss problem using different values of  $\theta$  and constraint handling methods

BCH method	$\theta$ value									Range (%)
	0	0.25	0.5	0.75	1	2	3	4	6	
Absorbing	566.349	542.753	542.516	541.190	540.655	539.105	540.853	544.308	554.803	5.054
Random	572.832	565.346	563.810	562.044	562.719	554.882	550.694	550.736	550.528	4.051
Random_all	564.585	566.579	567.869	572.264	567.630	566.559	564.775	562.186	560.383	2.120
Conservation	561.306	543.764	542.948	541.400	541.332	540.169	539.927	540.866	541.593	3.960
Infinity	565.915	545.717	542.937	539.820	541.489	551.027	568.085	577.171	576.258	6.919
Periodic	563.376	563.615	563.652	564.908	563.189	557.340	555.919	552.426	550.240	2.666
Mirror	561.648	545.289	544.619	541.834	541.916	540.568	540.216	539.910	540.529	4.026
EBCH	565.790	544.974	542.795	541.703	541.105	539.853	540.048	540.054	542.316	4.804
Exp-C	560.801	545.959	543.653	543.414	543.001	540.626	540.870	540.866	542.677	3.732
Exp-S	567.173	566.395	562.563	562.147	561.217	555.856	552.426	549.447	551.992	3.226
IP-C	565.437	544.155	542.089	541.419	543.266	539.696	541.293	539.468	541.840	4.814
IP-S	562.292	547.352	549.774	549.553	549.772	545.254	544.340	545.609	545.035	3.298
PEBCH	566.679	544.094	542.799	541.318	541.043	539.943	538.890	540.454	540.964	5.157
Flyback	554.331	542.536	540.865	540.432	540.618	539.878	538.746	538.206	539.671	2.996
Flyback-best	557.220	543.225	541.591	540.250	540.053	538.142	<b>538.079</b>	539.191	539.831	3.557

Periodic, Mirror, Exp-S, and IP-S. Results using the remaining BCH methods are visualized in Figure 3. Upon applying this filter, from Table 2, it can be seen that the total variation of mean values for  $\theta$  between 0.75 and 3 are 0.38%, 0.27%, 0.34%, 0.52%, 0.66%, 0.45%, 0.34%, and 0.40% for Absorbing, Conservation, EBCH, EXP-C, IP-C, PEBCH, Flyback, and Flyback-best methods, respectively. Figure 3 shows that the Flyback-best method with  $\theta$  of 3 and 2, and Flyback with  $\theta = 4$  are the most efficient methods.

Convergence rate plots for mean values of the filtered BCH methods when  $\theta = 2$  are compared in Figure 4. We selected  $\theta = 2$  because most of the BCH methods performed better with this value for this case. As can be seen in Figure 4, there is no considerable difference between convergence trends of different methods. However, PEBCH converged slightly faster than the other methods.

To achieve a better understanding of the impact of each BCH method on the performance of the algorithm, information on population diversity is provided in Figures 5 and 6. Figure 5 shows a full comparison of population diversity for all the methods with  $\theta = 2$ , and Figure 6 shows the diversity measures of the filtered methods. We can see in Figure 5 that all the methods except Random-all started their search with their highest level of diversification and followed a decreasing

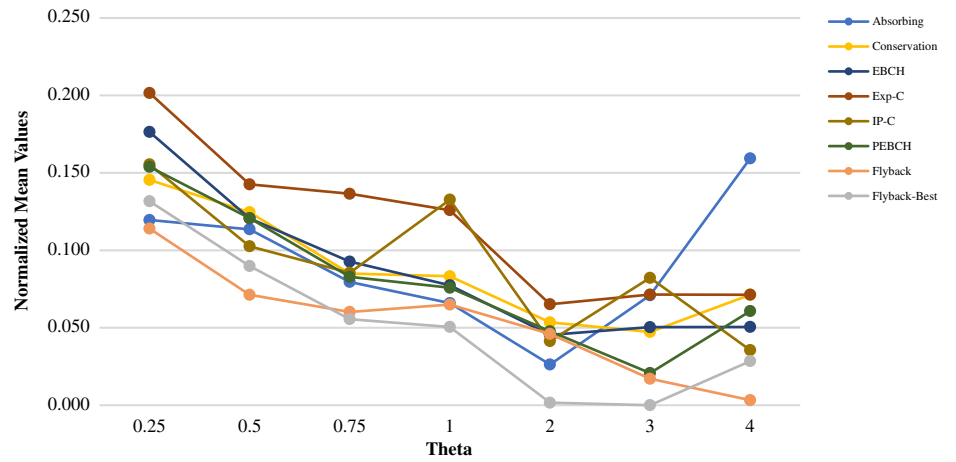
TABLE 3 Normalized best values for 10-bar 2-D truss

BCH method	$\theta$ value									$\Sigma$
	0	0.25	0.5	0.75	1	2	3	4	6	
Absorbing	0.531	0.077	0.074	0.089	0.079	0.084	0.127	0.093	0.402	1.556
Random	0.589	0.439	0.650	0.690	0.439	0.555	0.248	0.282	0.230	4.121
Random_all	0.292	0.681	0.497	0.906	0.536	0.532	0.415	0.695	0.443	4.996
Conservation	0.243	0.115	0.052	0.106	0.087	0.044	0.051	0.054	0.037	0.790
Infinity	0.404	0.185	0.219	0.091	0.074	0.281	0.689	0.656	<b>1.000</b>	3.599
Periodic	0.289	0.418	0.458	0.365	0.451	0.273	0.310	0.213	0.325	3.103
Mirror	0.407	0.175	0.079	0.102	0.128	0.043	<b>0.000</b>	0.020	0.073	1.026
EBCH	0.357	0.104	0.033	0.035	0.056	0.082	0.085	0.064	0.135	0.951
Exp-C	0.359	0.118	0.081	0.058	0.095	0.107	0.053	0.051	0.112	1.034
Exp-S	0.550	0.501	0.531	0.622	0.344	0.663	0.540	0.166	0.292	4.210
IP-C	0.473	0.179	0.094	0.071	0.067	0.063	0.053	0.076	0.044	1.121
IP-S	0.581	0.275	0.244	0.329	0.112	0.068	0.166	0.142	0.228	2.145
PEBCH	0.440	0.074	0.069	0.033	0.069	0.046	0.032	0.028	0.086	0.876
Flyback	0.443	0.039	0.054	0.078	0.133	0.088	0.017	0.060	0.055	0.967
Flyback-best	0.148	0.034	0.162	0.059	0.065	0.025	0.023	0.029	0.050	<b>0.595</b>
$\Sigma$	6.105	3.415	3.298	3.632	2.735	2.953	2.810	<b>2.630</b>	3.512	-

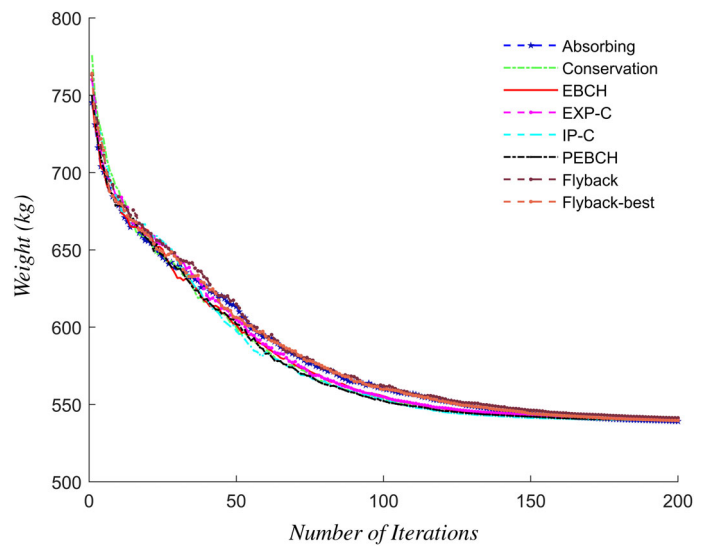
TABLE 4 Normalized mean values for 10-bar 2-D truss

BCH method	$\theta$ value									$\Sigma$
	0	0.25	0.5	0.75	1	2	3	4	6	
Absorbing	0.723	0.120	0.114	0.080	0.066	0.026	0.071	0.159	0.428	1.786
Random	0.889	0.698	0.658	0.613	0.630	0.430	0.323	0.324	0.318	4.883
Random_all	0.678	0.729	0.762	0.874	0.756	0.729	0.683	0.617	0.571	6.398
Conservation	0.594	0.145	0.125	0.085	0.083	0.053	0.047	0.071	0.090	1.294
Infinity	0.712	0.195	0.124	0.045	0.087	0.331	0.768	<b>1.000</b>	0.977	4.239
Periodic	0.647	0.653	0.654	0.686	0.642	0.493	0.456	0.367	0.311	4.910
Mirror	0.603	0.184	0.167	0.096	0.098	0.064	0.055	0.047	0.063	1.377
EBCH	0.709	0.176	0.121	0.093	0.077	0.045	0.050	0.051	0.108	1.431
Exp-C	0.581	0.202	0.143	0.136	0.126	0.065	0.071	0.071	0.118	1.513
Exp-S	0.744	0.724	0.626	0.616	0.592	0.455	0.367	0.291	0.356	4.771
IP-C	0.700	0.155	0.103	0.085	0.133	0.041	0.082	0.036	0.096	1.431
IP-S	0.619	0.237	0.299	0.294	0.299	0.184	0.160	0.193	0.178	2.463
PEBCH	0.732	0.154	0.121	0.083	0.076	0.048	0.021	0.061	0.074	1.368
Flyback	0.416	0.114	0.071	0.060	0.065	0.046	0.017	0.003	0.041	<b>0.833</b>
Flyback-best	0.490	0.132	0.090	0.056	0.051	0.002	<b>0.000</b>	0.028	0.045	0.892
$\Sigma$	9.837	4.619	4.177	3.901	3.781	3.011	3.172	3.318	3.773	

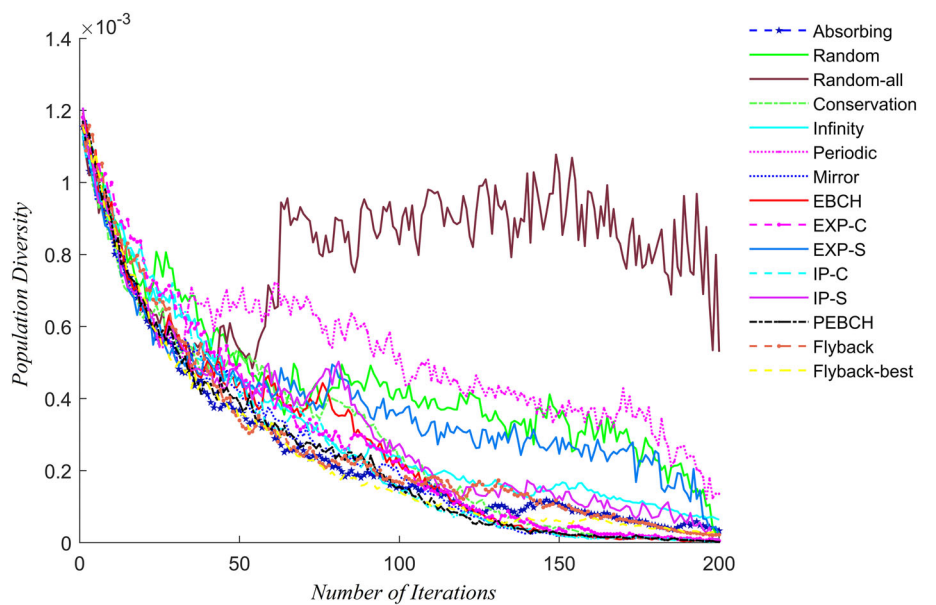
**FIGURE 3** Comparison of filtered normalized mean values for 10-bar 2-D truss



**FIGURE 4** Convergence rates of different BCH methods for 10-bar 2-D truss



**FIGURE 5** Population diversity of all the BCH methods for the 10-bar truss problem



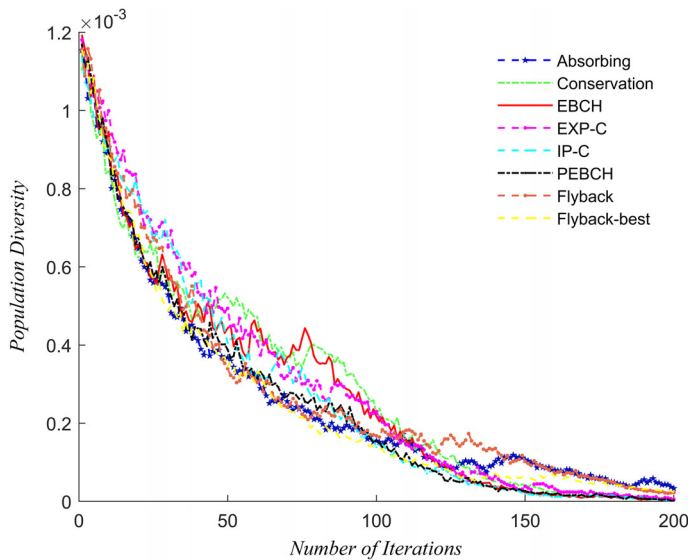


FIGURE 6 Population diversity of the filtered BCH methods for the 10-bar truss problem

TABLE 5 Comparison of optimization results for the 10-bar truss problem

Design variables	Sedaghati et al <sup>34</sup>	Kaveh and Javadi <sup>36</sup>	Kaveh and Zolghadr <sup>35</sup>	Farshchin et al <sup>40</sup> (TLBO)	Farshchin et al <sup>40</sup> (MC-TLBO)	ISA (Mirror, $\theta = 3$ )
$A_1$ (cm <sup>2</sup> )	38.245	35.54	35.944	36.0171	35.8507	34.8912
$A_2$ (cm <sup>2</sup> )	9.916	9.916	15.53	15.0926	14.8424	15.9940
$A_3$ (cm <sup>2</sup> )	38.619	35.784	32.285	35.1797	35.5768	37.6089
$A_4$ (cm <sup>2</sup> )	18.232	14.606	15.385	14.8551	14.9305	15.3634
$A_5$ (cm <sup>2</sup> )	4.419	0.646	0.648	0.6495	0.645	0.0059
$A_6$ (cm <sup>2</sup> )	4.194	4.626	4.583	4.6192	4.6249	4.7684
$A_7$ (cm <sup>2</sup> )	20.097	24.779	23.61	24.2147	23.9816	23.6343
$A_8$ (cm <sup>2</sup> )	24.097	23.31	23.599	23.8069	24.2358	23.3212
$A_9$ (cm <sup>2</sup> )	13.89	12.482	13.135	12.9309	12.6977	12.7561
$A_{10}$ (cm <sup>2</sup> )	11.4516	12.675	12.357	12.3585	12.3319	12.0052
Weight (kg)	537.01	532.11	532.39	532.136	532.051	532.0444
Mean (kg)	NA	NA	537.8	535.119	533.232	540.216
SD (kg)	NA	2.37	4.02	3.219	2.179	3.599
$f_1$	6.992	6.999	7.000	7.000	7.000	7.000
$f_2$	17.599	16.175	16.187	16.178	16.184	15.460
$f_3$	19.973	19.999	20.000	20.000	20.000	20.000
Constraint 1	NA	NA	NA	NA	NA	-0.0005
Constraint 2	NA	NA	NA	NA	NA	-0.4602
Constraint 3	NA	NA	NA	NA	NA	-0.0007

pattern while concentrating more on intensification. Periodic, Random, and EXP-S focused more on exploration than the other methods, until the final iterations. Figure 6 demonstrates that among the filtered methods, Absorbing provided the least diversification in the first 100 iterations, but provided the most diversification in the final 50 iterations. In addition, we can see in Figure 6 that the search domain space in EBCH, Conservation, and PEBCH is larger than other methods; this space shrunk as those algorithms approached their final iterations.

Table 5 compares the best solution obtained in this study with data available in the literature. It can be seen that the best solution obtained using the ISA corresponds to the lowest overall structural weight. However, in terms of mean values, this algorithm could not outperform the other methods under comparison.

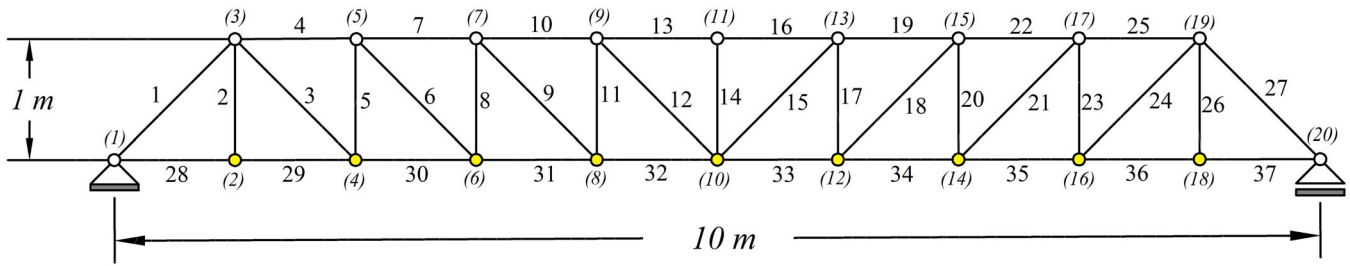


FIGURE 7 Schematic of the planar 37-bar truss structure showing the initial layout of the truss

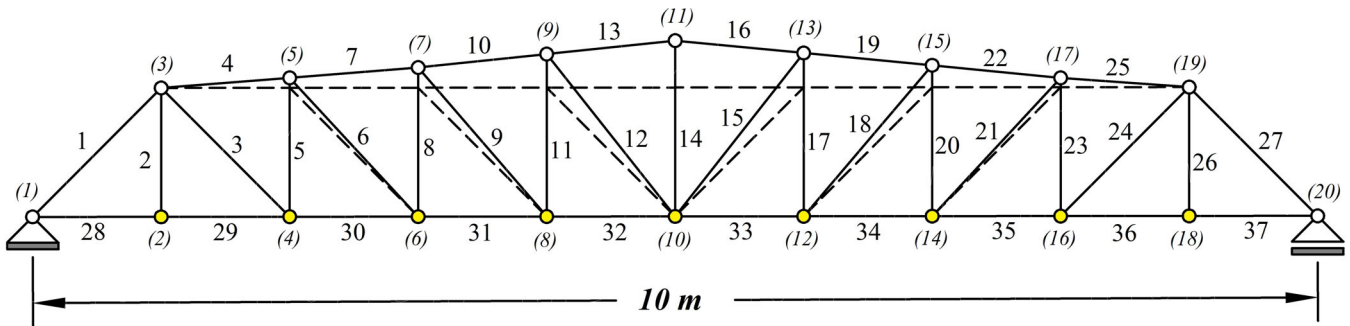


FIGURE 8 Optimized layout of the planar 37-bar truss structure

TABLE 6 Design parameters of planar 37-bar truss

Property	Value (unit)
Modulus of elasticity ( $E$ )	$2.1 \times 10^{11}$ (N/m <sup>2</sup> )
Material density ( $\rho$ )	7800 (kg/m <sup>3</sup> )
Design variable lower bound	$1 \times 10^{-4}$ (m <sup>2</sup> )
Design variable upper bound	$10 \times 10^{-4}$ (m <sup>2</sup> )
Frequency constraints	$f_1 \geq 20, f_2 \geq 40, f_3 \geq 60$ (Hz)

### 5.1.2 | Planar 37-bar truss

The weight minimization of the 37-bar planar truss structure shown in Figure 7, has been previously tackled by Sedaghati et al.,<sup>34</sup> Gomes<sup>37</sup> and Miguel and Miguel.<sup>38</sup> In this problem, the main objective is the optimum design of size as well as the vertical position of nodes on the upper chord as shown in Figure 8. The essential parameters to describe this case study are provided in Table 6. A non-structural mass equal to 10 kg is added to all the free nodes on the lower chord. Moreover, all the elements along the lower chord have a constant cross-sectional area of  $4 \times 10^{-3}$  m<sup>2</sup>.

The average values of optimized weight obtained for this case study are summarized in Table 7. Furthermore, the normalized best and mean results are presented in Tables 8 and 9, respectively. The lowest best value was obtained by the PEBCH approach with  $\theta = 1$ . The minimum cumulative values based on the normalized best values were obtained with the Conservation BCH method, and this value is minimum for  $\theta = 3$ . Regarding the mean values, it can be seen in Table 9 that Absorbing with  $\theta = 2$ , EBCH with  $\theta = 2$ , and Flyback-best with  $\theta$  values of 1 and 2 provided the lowest normalized mean value. Similarly, the least cumulative normalized mean value was obtained with the PEBCH approach and for  $\theta = 2$ . The same set of BCH methods was used as in the previous example to generate Figure 9, which compares the normalized mean values of the selected methods. It can be seen from Figure 9 that the best BCH methods for the 37-bar truss case were Flyback-best with  $\theta = 1$ . Moreover, the other methods performed most efficiently with  $\theta = 2$ . We can also see from Table 7 that the total variations of mean values for  $\theta$  between 0.75 and 3 are 0.030%, 0.030%, 0.034%,

**TABLE 7** Mean values of the optimized weight obtained for the 37-bar truss problem using different values of  $\theta$  and constraint handling methods

BCH method	$\theta$ value									Range (%)
	0	0.25	0.5	0.75	1	2	3	4	6	
Absorbing	354.479	352.434	352.349	352.388	352.297	352.282	352.383	352.334	352.482	0.624
Random	379.332	384.521	377.601	377.090	374.519	370.723	370.262	369.419	369.854	4.088
Random_all	364.693	364.371	364.739	364.121	364.463	364.641	365.154	366.036	365.678	0.526
Conservation	354.829	352.459	352.467	352.377	352.372	352.303	352.311	352.410	352.450	0.717
Infinity	375.029	371.631	367.952	365.533	363.668	359.397	359.301	357.826	359.118	4.807
Periodic	381.259	387.520	381.787	378.392	374.766	367.786	365.017	364.228	367.163	6.395
Mirror	383.813	377.552	368.429	363.523	361.547	360.277	362.280	363.995	366.309	6.533
EBCH	354.781	352.391	352.420	352.335	352.292	352.276	352.326	352.395	352.456	0.711
Exp-C	354.649	352.647	352.654	352.482	352.522	352.504	352.580	352.580	352.609	0.615
Exp-S	380.881	380.062	378.067	370.756	365.503	363.123	364.599	364.849	366.051	4.890
IP-C	354.517	352.605	352.491	352.447	352.543	352.465	352.477	352.463	352.600	0.587
IP-S	358.705	362.059	366.185	364.311	361.060	360.538	360.187	359.522	359.847	2.085
PEBCH	354.143	352.351	352.359	352.337	352.424	352.294	352.362	352.380	352.407	0.525
Flyback	355.764	353.726	353.266	353.223	352.917	352.737	352.724	353.528	352.953	0.862
Flyback-best	354.395	352.454	352.327	352.323	<b>352.267</b>	352.280	352.340	353.082	352.441	0.604

**TABLE 8** Normalized best values for 37-bar 2-D truss

BCH method	$\theta$ value									$\Sigma$
	0	0.25	0.5	0.75	1	2	3	4	6	
Absorbing	0.016	0.002	0.002	0.002	0.004	0.002	0.002	0.004	0.004	0.039
Random	0.618	0.159	0.536	0.489	0.323	0.436	0.437	0.353	0.422	3.773
Random_all	0.312	0.272	0.365	0.308	0.383	0.357	0.349	0.428	0.348	3.122
Conservation	0.015	0.002	0.001	0.001	0.003	0.002	0.003	0.001	0.003	<b>0.033</b>
Infinity	0.368	0.051	0.115	0.125	0.205	0.097	0.095	0.046	0.087	1.189
Periodic	0.885	<b>1.000</b>	0.611	0.914	0.432	0.318	0.189	0.188	0.382	4.920
Mirror	0.536	0.417	0.247	0.070	0.181	0.127	0.177	0.226	0.269	2.252
EBCH	0.018	0.003	0.006	0.002	0.003	0.003	0.002	0.003	0.005	0.044
Exp-C	0.021	0.004	0.009	0.007	0.004	0.004	0.013	0.007	0.008	0.078
Exp-S	0.490	0.460	0.343	0.267	0.244	0.173	0.187	0.242	0.284	2.690
IP-C	0.018	0.006	0.004	0.003	0.011	0.007	0.007	0.005	0.014	0.074
IP-S	0.112	0.163	0.162	0.206	0.157	0.130	0.046	0.164	0.124	1.264
PEBCH	0.027	0.003	0.002	0.001	<b>0.000</b>	0.001	0.002	0.005	0.004	0.043
Flyback	0.063	0.023	0.021	0.017	0.012	0.018	0.015	0.014	0.010	0.193
Flyback-best	0.028	0.003	0.003	0.001	0.002	0.001	0.001	0.003	0.007	0.049
$\Sigma$	3.527	2.568	2.430	2.413	1.964	1.676	<b>1.524</b>	1.689	1.973	-

TABLE 9 Normalized mean values for 37-bar 2-D truss

BCH method	$\theta$ value									$\Sigma$
	0	0.25	0.5	0.75	1	2	3	4	6	
Absorbing	0.063	0.005	0.002	0.003	0.001	0.000	0.003	0.002	0.006	0.086
Random	0.768	0.915	0.719	0.704	0.631	0.524	0.510	0.487	0.499	5.756
Random_all	0.352	0.343	0.354	0.336	0.346	0.351	0.366	0.391	0.380	3.219
Conservation	0.073	0.005	0.006	0.003	0.003	0.001	0.001	0.004	0.005	0.101
Infinity	0.646	0.549	0.445	0.376	0.323	0.202	0.200	0.158	0.194	3.093
Periodic	0.822	<b>1.000</b>	0.837	0.741	0.638	0.440	0.362	0.339	0.423	5.603
Mirror	0.895	0.717	0.458	0.319	0.263	0.227	0.284	0.333	0.398	3.895
EBCH	0.071	0.004	0.004	0.002	0.001	0.000	0.002	0.004	0.005	0.093
Exp-C	0.068	0.011	0.011	0.006	0.007	0.007	0.009	0.009	0.010	0.137
Exp-S	0.812	0.788	0.732	0.524	0.375	0.308	0.350	0.357	0.391	4.637
IP-C	0.064	0.010	0.006	0.005	0.008	0.006	0.006	0.006	0.009	0.119
IP-S	0.183	0.278	0.395	0.342	0.249	0.235	0.225	0.206	0.215	2.326
PEBCH	0.053	0.002	0.003	0.002	0.004	0.001	0.003	0.003	0.004	<b>0.075</b>
Flyback	0.099	0.041	0.028	0.027	0.018	0.013	0.013	0.036	0.019	0.296
Flyback-best	0.060	0.005	0.002	0.002	<b>0.000</b>	0.000	0.002	0.023	0.005	0.099
$\Sigma$	5.028	4.674	4.002	3.393	2.869	<b>2.315</b>	2.334	2.356	2.565	-

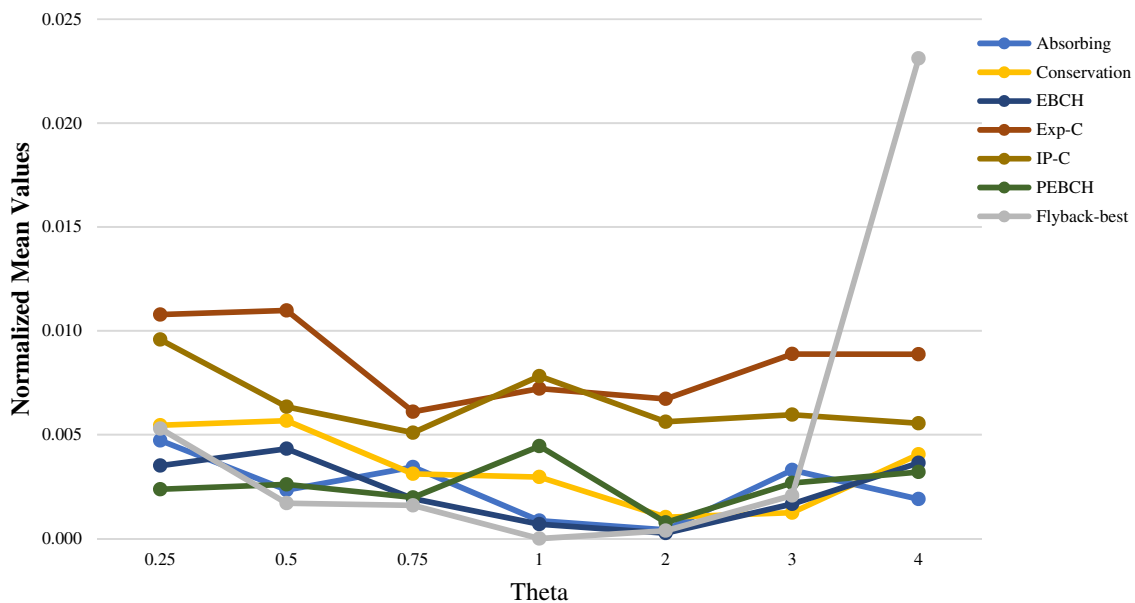


FIGURE 9 Comparison of filtered normalized mean values for 37-bar 2-D truss

0.028%, 0.027%, 0.037%, 0.228%, and 0.231% for Absorbing, Conservation, EBCH, EXP-C, IP-C, PEBCH, Flyback, and Flyback-best methods, respectively.

The mean convergence rates of the six selected BCH methods, based on the filtering mentioned above, are compared in Figure 10. It is apparent that there is no considerable difference between the convergence trends of these BCH methods for the 37-bar problem.

Population diversity measures for all the BCH methods, as well as the six best methods with  $\theta = 2$ , are shown in Figures 11 and 12, respectively. As seen in Figure 11, Random, Random-all, IP-S, EXP-S, and EXP-C concentrated on



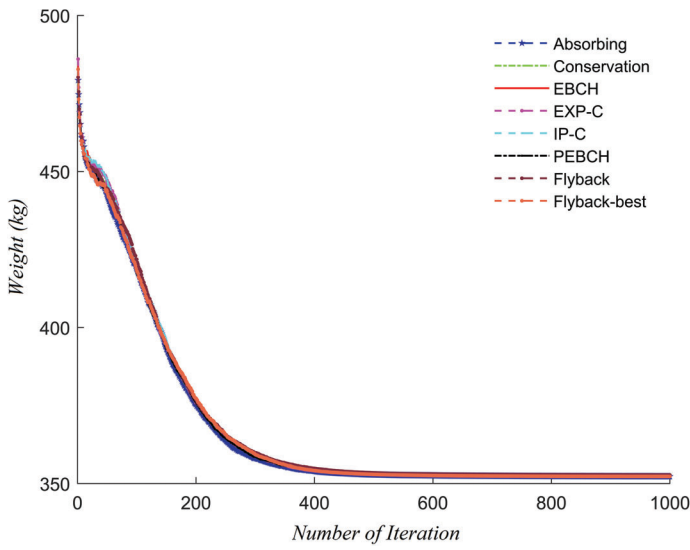


FIGURE 10 Convergence rates of different BCH methods for the 37-bar truss problem

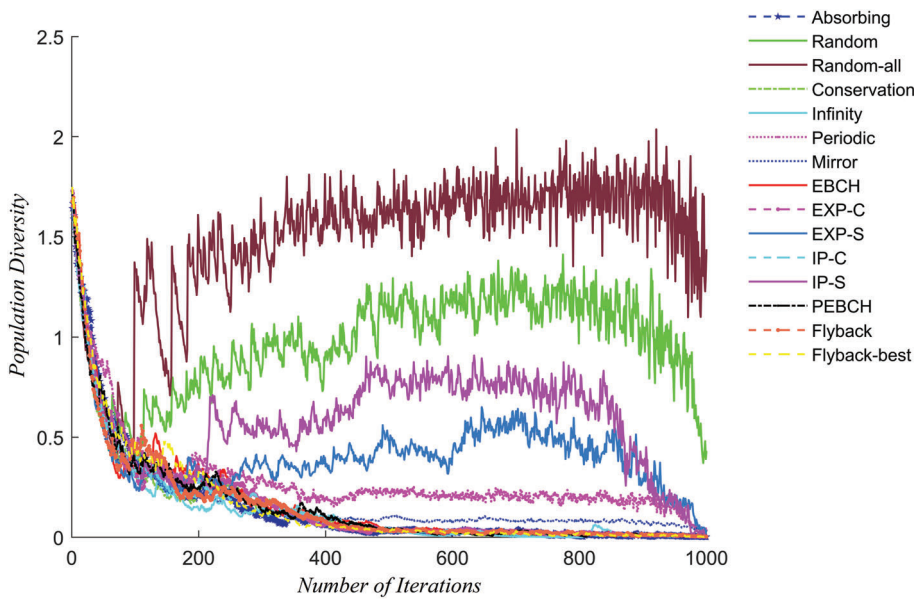


FIGURE 11 Population diversity of all the BCH methods for the 37-bar truss problem

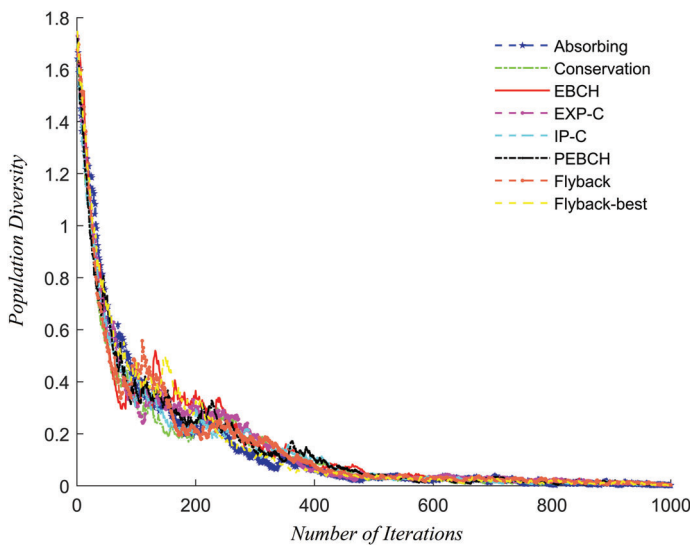


FIGURE 12 Population diversity of the filtered BCH methods for the 37-bar truss problem



diversification rather than intensification during the course of the iterations. We can also see that the search domain for these methods is wider than for the other methods. The remaining BCH methods presented higher diversification during the initial iterations and focused on intensification during the later iterations. Figure 12 shows that, similar to the previous design example, EBCH, Conservation, and PEBCH provide more distance between the two ends of the search space.

The best solution obtained by the ISA is compared with those from the literature in Table 10. It can be seen that, overall, the ISA is the best algorithm.

### 5.1.3 | Spatial 52-bar truss

Figures 13 and 14 show the spatial 52-bar truss structure proposed by Lin et al.<sup>43</sup> In this problem, the goal is to optimize the size and the shape of the truss structure. To this end, the structural elements are divided into eight different groups. Free nodes are allowed to move  $\pm 2$  m from their original position in both radial and vertical directions to preserve the radial symmetry of the structure. A non-structural mass equal to 50 kg is added to each free node as shown in Figures 13 and 14. The essential parameters for describing this case study are listed in Table 11.

The average optimized weights over 50 independent runs are listed in Table 12. The normalized best and mean results are also presented in Tables 13 and 14, respectively. It can be seen from Table 13 that the Absorbing method with  $\theta = 2$  has the lowest objective value. The minimum cumulative best value was obtained by the Absorbing method and, in terms of  $\theta$ , the minimum cumulative best value was obtained with  $\theta = 0.5$ . We can see from Table 14 that the minimum cumulative mean value was obtained by EBCH and this cumulative value was minimum for  $\theta = 3$ . The lowest mean value was recorded by PEBCH with  $\theta = 2$ . The same methods filtered previously were selected to compare the normalized mean values, as shown in Figure 15. It appears that EBCH and PEBCH perform better than the other methods with lower mean values. Moreover, the ISA with different BCH methods performs better when  $\theta$  varies between 0.75 and 2. The range of variations for the objective values when  $\theta$  is between 0.75 and 3 are 4.472%, 1.572%, 4.907%, 4.332%, 4.838%, 4.693%, 4.927%, and 5.305% for Absorbing, Conservation, EBCH, EXP-C, IP-C, PEBCH, Flyback, and Flyback-best methods, respectively.

A convergence rate plot based on the mean values for  $\theta = 3$  is presented for the selected BCH methods in Figure 16, and in this case, no significant difference between the different methods is observed.

A comparison of the best solution obtained in this study with previous solutions from the literature is provided in Table 15. We can see that, for this case study, the ISA achieved lower objective values than all methods, with the exception of Farshchin et al.<sup>40</sup>

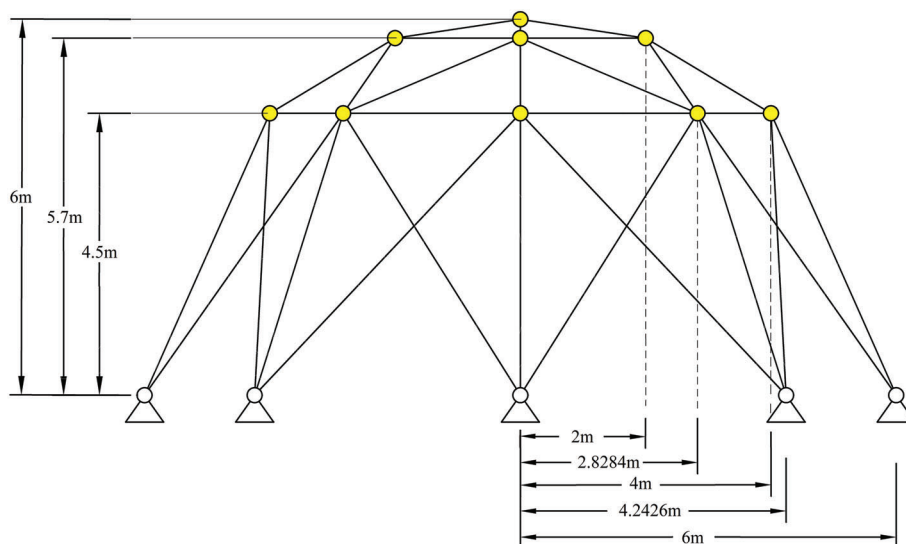
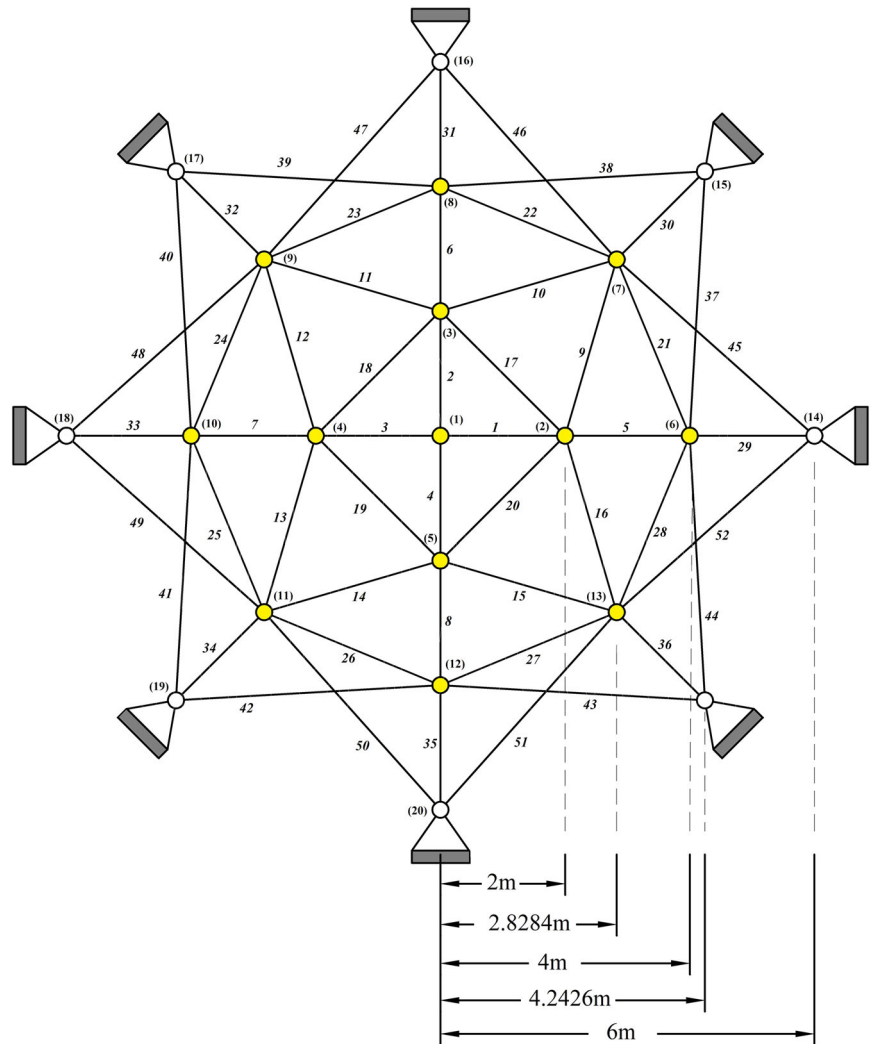


FIGURE 13 Initial layout of the spatial 52-bar truss structure

**FIGURE 14** Top view of the spatial 52-bar truss structure including numbering of elements and nodes



**TABLE 11** Design parameters of the spatial 52-bar truss

Property	Value (unit)
Modulus of elasticity ( $E$ )	$2.1 \times 10^{11}$ (N/m <sup>2</sup> )
Material density ( $\rho$ )	7800 (kg/m <sup>3</sup> )
Design variable lower bound	$1 \times 10^{-4}$ (m <sup>2</sup> )
Design variable upper bound	$10 \times 10^{-4}$ (m <sup>2</sup> )
Frequency constraints	$f_1 \leq 15.916, f_2 \geq 28.648$ (Hz)

Population diversity variations are depicted in Figures 17 and 18 for all the BCH methods and for filtered methods with  $\theta = 3$ , respectively. We can see from Figure 17 that, similar to the previous case studies, Random-all pushes the algorithm toward diversification rather than intensification. Although Random, Periodic, Mirror, and IP-S methods moved from diversification to intensification in the final iterations, their diversification was higher than the other algorithms. Moreover, in the above mentioned BCH methods as well as the Random-all method, the size of the search space is larger than the other methods. Figure 18 shows that the filtered BCH methods gradually switch from higher diversification in the initial steps to higher intensification around the 400th iterations. Between the 400th to 600th iterations an abrupt increase was observed for all the BCH methods and the diversity decreased gradually after the 600th iterations.

**TABLE 12** Mean values of the optimized weight obtained for the 52-bar truss problem using different values of  $\theta$  and constraint handling methods

BCH method	$\theta$ value									Range (%)
	0	0.25	0.5	0.75	1	2	3	4	6	
Absorbing	267.364	211.298	206.247	206.448	200.789	203.982	209.767	201.246	206.307	33.157
Random	298.498	303.741	274.869	278.168	288.043	303.535	304.480	302.416	301.506	10.773
Random_all	257.453	246.718	244.838	244.605	246.342	253.398	270.636	269.165	269.518	10.642
Conservation	250.714	219.505	206.869	204.993	202.040	203.418	203.868	205.217	206.824	24.091
Infinity	294.715	260.221	241.372	240.298	226.918	229.001	217.362	224.108	224.101	35.587
Periodic	297.440	297.641	292.421	297.143	302.790	283.112	254.172	250.301	249.942	21.144
Mirror	312.848	283.014	275.643	251.986	247.953	229.159	238.759	233.504	247.905	36.520
EBCH	259.544	206.664	206.432	203.132	199.331	200.425	204.043	209.112	206.383	30.207
Exp-C	250.385	214.243	210.286	202.739	202.238	203.552	209.418	210.999	206.848	23.807
Exp-S	323.731	313.632	293.604	293.923	300.480	300.037	290.623	302.385	315.625	11.392
IP-C	259.240	220.538	212.456	204.090	203.438	206.551	203.503	213.280	213.557	27.430
IP-S	279.522	267.307	263.534	256.193	257.478	257.345	246.717	253.812	266.542	13.296
PEBCH	277.442	214.435	205.576	202.926	200.281	<b>199.192</b>	208.541	207.926	217.400	39.283
Flyback	259.128	223.321	216.850	213.167	204.608	203.158	208.847	205.195	210.598	27.550
Flyback-best	275.793	211.441	205.495	203.132	201.534	201.876	205.130	212.225	207.631	36.847

**TABLE 13** Normalized best values for 52-bar 3-D truss

BCH method	$\theta$ value									$\Sigma$
	0	0.25	0.5	0.75	1	2	3	4	6	
Absorbing	0.017	0.001	0.003	0.007	0.002	<b>0.000</b>	0.012	0.003	0.009	<b>0.054</b>
Random	0.497	0.712	0.146	0.200	0.464	0.469	0.403	0.441	0.564	3.897
Random_all	0.475	0.532	0.275	0.489	0.155	0.364	0.349	0.492	0.696	3.827
Conservation	0.103	0.005	0.007	0.008	0.005	0.005	0.005	0.010	0.010	0.158
Infinity	0.309	0.250	0.173	0.143	0.099	0.145	0.063	0.065	0.059	1.305
Periodic	0.382	0.710	0.390	0.823	1.000	0.271	0.173	0.229	0.219	4.197
Mirror	0.794	0.456	0.100	0.167	0.140	0.174	0.160	0.170	0.096	2.256
EBCH	0.118	0.006	0.003	0.007	0.006	0.002	0.004	0.010	0.019	0.175
Exp-C	0.120	0.025	0.015	0.021	0.013	0.010	0.001	0.004	0.008	0.217
Exp-S	0.828	0.470	0.566	0.630	0.548	0.951	0.881	0.496	0.696	6.065
IP-C	0.118	0.017	0.016	0.004	0.011	0.005	0.007	0.015	0.010	0.205
IP-S	0.241	0.255	0.322	0.317	0.220	0.191	0.130	0.399	0.217	2.292
PEBCH	0.015	0.003	0.014	0.003	0.002	0.005	0.009	0.017	0.015	0.083
Flyback	0.184	0.048	0.035	0.072	0.021	0.014	0.017	0.030	0.038	0.459
Flyback-best	0.074	0.009	0.006	0.006	0.016	0.006	0.007	0.009	0.022	0.155
$\Sigma$	4.276	3.500	<b>2.070</b>	2.896	2.701	2.613	2.219	2.392	2.678	-

TABLE 14 Normalized mean values for 52-bar 3-D truss

BCH method	$\theta$ value									$\Sigma$
	0	0.25	0.5	0.75	1	2	3	4	6	
Absorbing	0.547	0.097	0.057	0.058	0.013	0.038	0.085	0.016	0.057	0.969
Random	0.797	0.839	0.608	0.634	0.713	0.838	0.845	0.829	0.822	6.926
Random_all	0.468	0.382	0.367	0.365	0.379	0.435	0.574	0.562	0.565	4.095
Conservation	0.414	0.163	0.062	0.047	0.023	0.034	0.038	0.048	0.061	0.889
Infinity	0.767	0.490	0.339	0.330	0.223	0.239	0.146	0.200	0.200	2.934
Periodic	0.789	0.791	0.749	0.787	0.832	0.674	0.441	0.410	0.407	5.880
Mirror	0.913	0.673	0.614	0.424	0.392	0.241	0.318	0.276	0.391	4.240
EBCH	0.485	0.060	0.058	0.032	0.001	0.010	0.039	0.080	0.058	<b>0.822</b>
Exp-C	0.411	0.121	0.089	0.028	0.024	0.035	0.082	0.095	0.061	0.947
Exp-S	<b>1.000</b>	0.919	0.758	0.761	0.813	0.810	0.734	0.829	0.935	7.558
IP-C	0.482	0.171	0.106	0.039	0.034	0.059	0.035	0.113	0.115	1.156
IP-S	0.645	0.547	0.517	0.458	0.468	0.467	0.382	0.439	0.541	4.462
PEBCH	0.628	0.122	0.051	0.030	0.009	<b>0.000</b>	0.075	0.070	0.146	1.132
Flyback	0.481	0.194	0.142	0.112	0.043	0.032	0.078	0.048	0.092	1.222
Flyback-best	0.615	0.098	0.051	0.032	0.019	0.022	0.048	0.105	0.068	1.056
$\Sigma$	9.442	5.668	4.566	4.136	3.986	3.933	<b>3.918</b>	4.119	4.519	-

FIGURE 15 Comparison of the filtered normalized mean values for the 52-bar truss problem

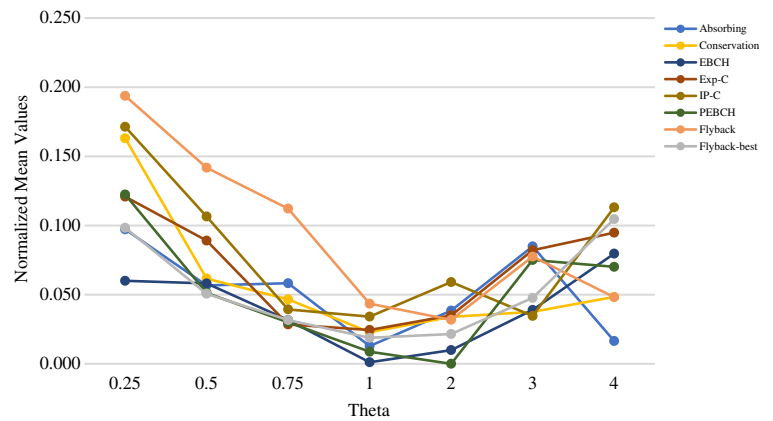
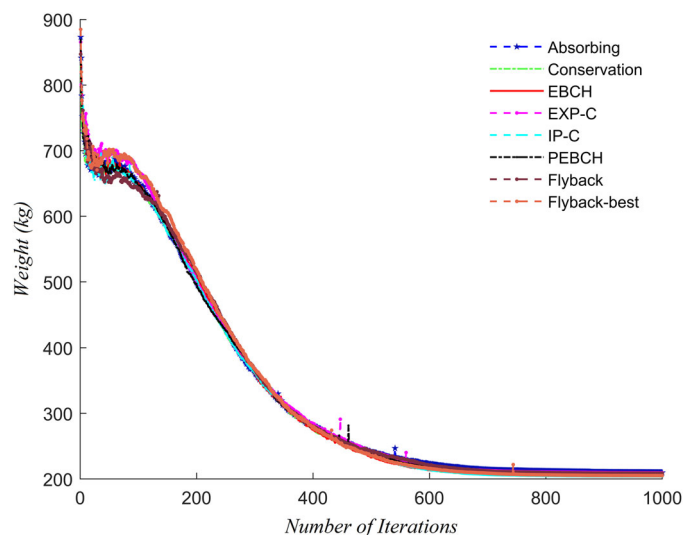


FIGURE 16 Convergence rates of different BCH methods for 52-bar 3-D truss







**FIGURE 17** Population diversity of all the BCH methods for 52-bar 3-D truss

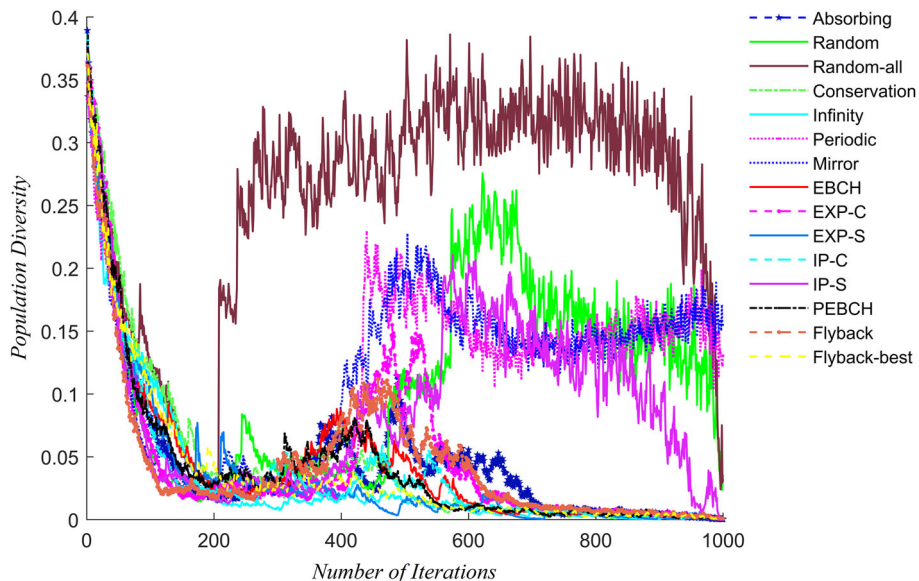
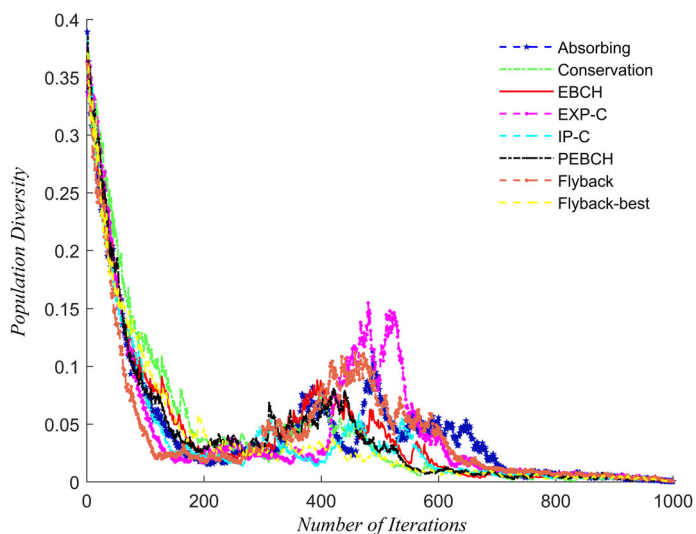


**FIGURE 18** Population diversity of the filtered BCH methods for 52-bar 3-D truss



#### 5.1.4 | Spatial 72-bar truss

The weight minimization problem of the spatial 72-bar truss structure shown in Figure 19 was previously solved by Miguel and Miguel<sup>38</sup> and Kaveh and Ghazaan.<sup>44</sup> The truss is designed using 16 groups of structural elements to maintain the structural symmetry. Four non-structural masses equal to 2268 kg are added to nodes 1–4. Descriptive parameters for this case study are provided in Table 16.

Average weights and normalized best and mean results are presented in Tables 17, 18, and 19, respectively. Based on the results, the Conservation method and  $\theta = 0.5$  provided the minimum mean value (about 331.4156). Moreover, we can see from Table 17 that the Conservation method and  $\theta = 0.25$  are the most efficient method and best parameter setting, respectively, based on their lowest cumulative normalized mean values. Similarly, the best-found solution was obtained by the Flyback-best method and  $\theta = 0.5$  (see Table 18). Figure 20 visually compares mean results using the same selection strategy adopted for the other design examples. We can see in Figure 20 that  $\theta = 0.25$  provided the best results considering most of the BCH schemes. Moreover, increasing  $\theta$  resulted in increasing the average weights. The mean values for the selected methods for  $\theta$  between 0.25 and 4 vary by about 21.64%, 25.31%, 26.65%, 24.51%, 24.15%, 25.56%, and 27.23% for Absorbing, Conservation, EBCH, EXP-C, IP-C, PEBCH, Flyback, and Flyback-best, respectively.

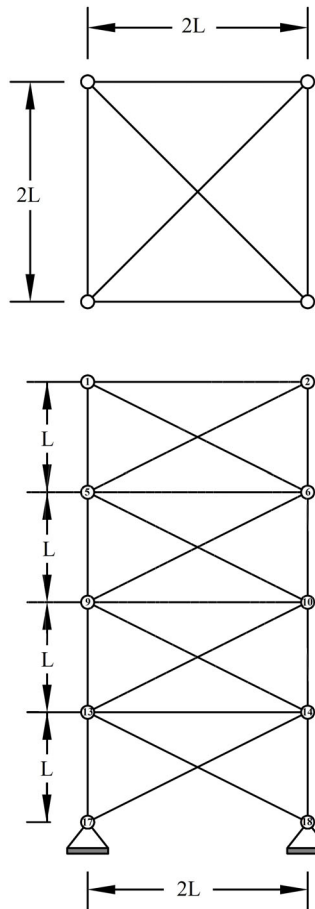
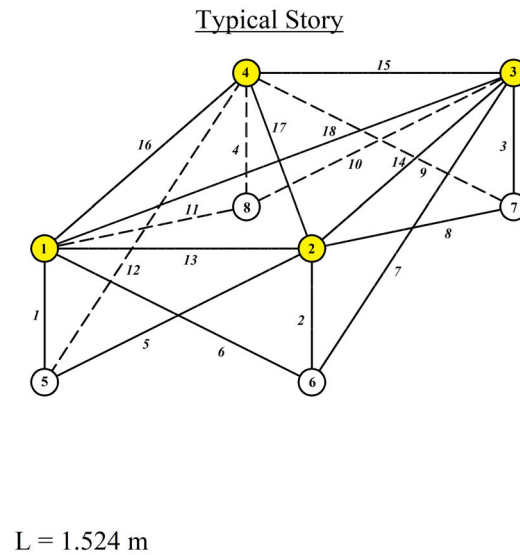


FIGURE 19 Schematic of the spatial 72-bar truss structure



Property	Value (unit)
Modulus of elasticity ( $E$ )	$6.895 \times 10^{10} \text{ (N/m}^2\text{)}$
Material density ( $\rho$ )	$2767.99 \text{ (kg/m}^3\text{)}$
Design variable lower bound	$6.45 \times 10^{-5} \text{ (m}^2\text{)}$
Design variable upper bound	$25 \times 10^{-4} \text{ (m}^2\text{)}$
Frequency constraints	$f_1 = 4, f_3 \geq 6 \text{ (Hz)}$

TABLE 16 Design parameters of the 72-bar 3-D truss

The mean convergence rates of the eight selected BCH methods for  $\theta = 0.25$  are compared in Figure 21. As seen in this figure, the best convergence was provided by Absorbing, EXP-C, and Flyback-best, in that order. The worst convergence was recorded by EBCH method in the 72-bar truss case. Conservation, PEBCH, and IP-C method were fairly poor compared to other selected methods in this case study.

We compare the population diversity of the utilized method when  $\theta = 0.25$  in Figures 22 and 23. Figure 22 shows that the Random-all scheme followed a pattern similar to the previous case studies. Random, Periodic, EXP-S, and IP-S methods provide stronger diversification than intensification. The remaining methods, as seen in Figure 23, started with stronger diversification and converged to focus more on intensification. It can also be observed in Figure 23 that EBCH searched through a wider solution space than the other methods, the Absorbing method provided more diversification during the final iterations, and PEBCH and IP-C had the most intensification during the final iterations.

The best solution with the ISA is compared with those from the literature in Table 20. Remarkably, the ISA converged to the lowest structural weight among all the compared methods. However, the constraints are slightly violated by the presented solution.

**TABLE 17** Mean values of the optimized weight obtained for the 72-bar truss problem using different values of  $\theta$  and constraint handling methods

BCH method	$\theta$ value									Range (%)
	0	0.25	0.5	0.75	1	2	3	4	6	
Absorbing	397.821	332.523	333.024	335.574	336.824	366.117	395.156	404.482	451.893	35.898
Random	491.845	476.907	482.839	485.128	490.738	525.787	522.050	527.744	539.764	13.180
Random_all	439.423	459.608	477.008	490.559	492.111	511.438	518.522	529.491	555.754	26.474
Conservation	390.225	333.838	<b>331.416</b>	335.912	336.455	363.357	387.149	415.286	459.563	38.667
Infinity	433.142	389.970	395.262	386.514	397.784	417.113	442.260	458.861	483.039	24.973
Periodic	448.163	462.789	469.575	466.416	479.267	506.438	520.271	526.246	529.042	18.047
Mirror	451.992	385.263	382.788	384.580	382.516	398.029	416.333	429.954	461.298	20.596
EBCH	392.317	335.192	333.538	337.471	337.254	365.113	388.231	422.417	466.475	39.856
Exp-C	382.694	341.024	350.518	354.890	358.661	382.684	406.056	424.614	448.302	31.458
Exp-S	512.528	485.332	494.227	484.613	493.109	511.526	518.878	526.840	534.985	10.394
IP-C	393.110	336.306	340.434	342.347	345.990	376.163	397.414	417.534	458.288	36.271
IP-S	400.745	413.162	428.285	444.073	435.713	465.803	474.727	490.137	485.122	22.306
PEBCH	392.358	331.777	333.513	338.000	347.206	356.298	385.218	415.167	460.303	38.739
Flyback	398.750	357.060	359.353	361.700	368.975	392.150	419.959	448.336	487.699	36.587
Flyback-best	399.357	331.533	333.059	334.236	338.707	356.166	398.410	421.800	449.017	35.437

**TABLE 18** Normalized best values for 72-bar 3-D truss

BCH method	$\theta$ value									$\Sigma$
	0	0.25	0.5	0.75	1	2	3	4	6	
Absorbing	0.151	0.003	0.002	0.002	0.003	0.027	0.082	0.032	0.246	<b>0.547</b>
Random	0.517	0.683	0.604	0.747	0.626	0.852	0.864	0.905	0.764	6.562
Random_all	0.440	0.523	0.582	0.635	0.608	0.848	0.627	<b>1.000</b>	0.974	6.237
Conservation	0.030	0.003	0.001	0.001	0.005	0.013	0.056	0.204	0.314	0.627
Infinity	0.261	0.200	0.046	0.140	0.186	0.262	0.404	0.437	0.553	2.488
Periodic	0.281	0.509	0.554	0.573	0.465	0.780	0.875	0.966	0.830	5.834
Mirror	0.358	0.101	0.122	0.166	0.088	0.119	0.184	0.334	0.518	1.990
EBCH	0.097	0.001	0.001	0.003	0.005	0.042	0.059	0.154	0.313	0.677
Exp-C	0.111	0.008	0.008	0.012	0.033	0.032	0.185	0.153	0.321	0.865
Exp-S	0.700	0.638	0.712	0.756	0.784	0.700	0.679	0.911	0.760	6.641
IP-C	0.089	0.001	0.004	0.006	0.006	0.072	0.072	0.127	0.313	0.689
IP-S	0.217	0.314	0.272	0.331	0.308	0.408	0.489	0.641	0.637	3.618
PEBCH	0.137	0.002	0.003	0.003	0.003	0.022	0.010	0.189	0.352	0.721
Flyback	0.209	0.060	0.072	0.056	0.025	0.144	0.231	0.402	0.647	1.847
Flyback-best	0.175	0.001	<b>0.000</b>	0.003	0.005	0.018	0.127	0.091	0.228	0.647
$\Sigma$	3.772	3.046	<b>2.984</b>	3.437	3.149	4.339	4.944	6.548	7.770	-

TABLE 19 Normalized mean values for 72-bar 3-D truss

BCH method	$\theta$ value									$\Sigma$
	0	0.25	0.5	0.75	1	2	3	4	6	
Absorbing	0.296	0.005	0.007	0.019	0.024	0.155	0.284	0.326	0.537	1.652
Random	0.715	0.649	0.675	0.685	0.710	0.866	0.850	0.875	0.929	6.954
Random_all	0.481	0.571	0.649	0.709	0.716	0.802	0.834	0.883	1.000	6.647
Conservation	0.262	0.011	0.000	0.020	0.022	0.142	0.248	0.374	0.571	1.651
Infinity	0.453	0.261	0.285	0.246	0.296	0.382	0.494	0.568	0.676	3.661
Periodic	0.520	0.586	0.616	0.602	0.659	0.780	0.842	0.868	0.881	6.354
Mirror	0.537	0.240	0.229	0.237	0.228	0.297	0.379	0.439	0.579	3.165
EBCH	0.271	0.017	0.009	0.027	0.026	0.150	0.253	0.406	0.602	1.762
Exp-C	0.229	0.043	0.085	0.105	0.121	0.229	0.333	0.415	0.521	2.080
Exp-S	0.807	0.686	0.726	0.683	0.721	0.803	0.836	0.871	0.907	7.040
IP-C	0.275	0.022	0.040	0.049	0.065	0.199	0.294	0.384	0.566	1.894
IP-S	0.309	0.364	0.432	0.502	0.465	0.599	0.639	0.708	0.685	4.703
PEBCH	0.272	0.002	0.009	0.029	0.070	0.111	0.240	0.373	0.575	1.681
Flyback	0.300	0.114	0.125	0.135	0.167	0.271	0.395	0.521	0.697	2.725
Flyback-best	0.303	0.001	0.007	0.013	0.033	0.110	0.299	0.403	0.524	1.692
$\Sigma$	6.032	3.571	3.894	4.060	4.324	5.897	7.219	8.414	10.249	-

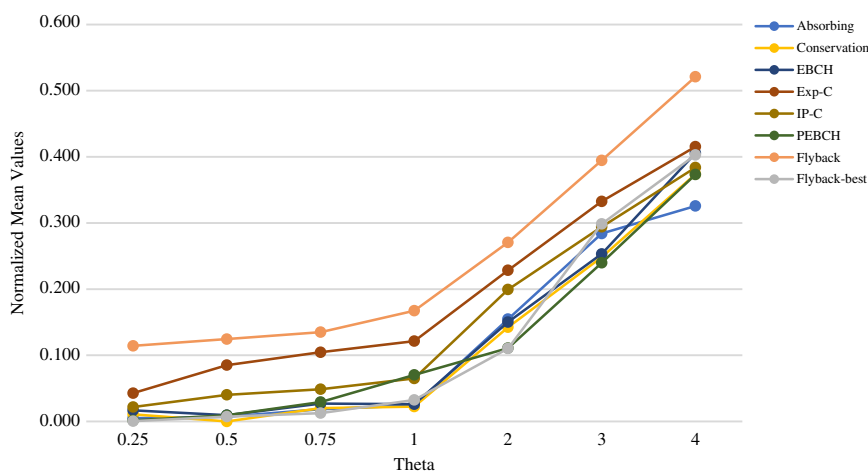


FIGURE 20 Comparison of the filtered normalized mean values for the 72-bar truss problem

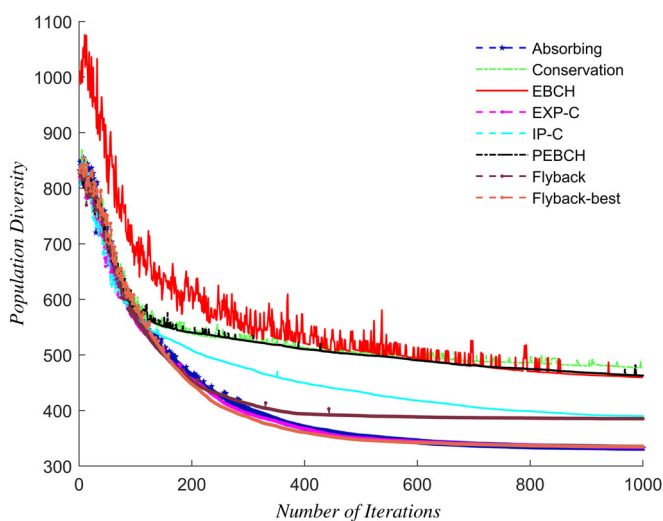
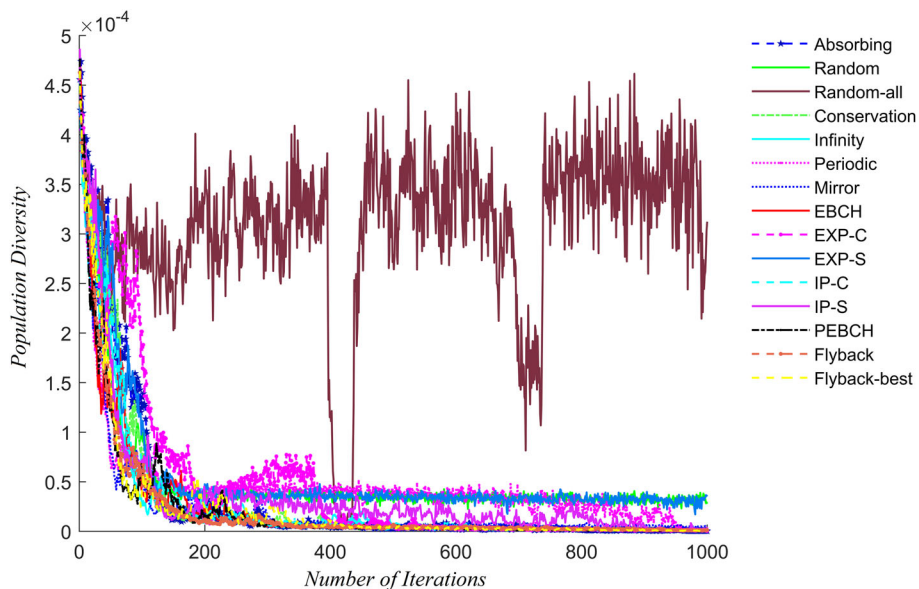
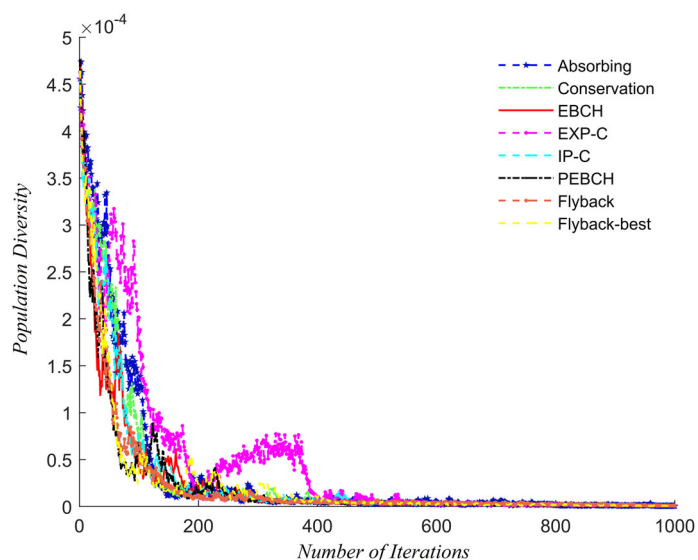


FIGURE 21 Convergence rates of different BCH methods for the 72-bar truss problem

**FIGURE 22** Population diversity of all the BCH methods for the 72-bar truss problem



**FIGURE 23** Population diversity of the filtered BCH methods for 72-bar 3-D truss



## 6 | CONCLUSION AND FUTURE WORK

In this study, different settings and variations of an art-inspired algorithm – the ISA – were applied on four benchmark truss optimization problems. In addition to automating the optimum design of truss structures using a robust and dependable optimization technique, this study also aimed to maximize the performance of ISA by applying and analyzing different configurations of the algorithm.

Specifically, adjusting the main parameter of the ISA through  $\theta$  for different truss problems and investigating the effect of various BCH approaches on the ISA were the main aims of this study. To explore the performance of all the variations, the benchmark truss problems were tackled using a combination of different  $\theta$  values (0, 0.25, 0.5, 0.75, 1, 2, 3, 4, and 6) and 13 different BCH schemes. We reported the results based on the best, mean and SD for 50 repeated runs of each combination. Moreover, the impact of different BCH methods on diversification and intensification was assessed by analyzing their population diversity. To this end, the  $L_1$  norm method was utilized to examine population diversity in each iteration.

The findings of this study clearly demonstrated the sensitivity of optimization results to the parameter  $\theta$ . Although it is possible to find a range of  $\theta$  that yields satisfactory results, this parameter should be tuned in order to maximize the

TABLE 20 Comparison of optimization results for the 72-bar truss problem

Design Variables	Elements	Miguel and Miguel <sup>38</sup>	Kaveh and Ghazaan <sup>44</sup>	Kaveh and Ghazaan <sup>45</sup>	Farshchin et al <sup>40</sup> (TLBO)	Farshchin et al <sup>40</sup> (MC-TLBO)	ISA (Flyback-best, $\theta = 0.5$ )
A <sub>1</sub> (cm <sup>2</sup> )	1–4	3.3411	3.5498	3.3437	3.54905	3.41877	3.7526
A <sub>2</sub> (cm <sup>2</sup> )	5–12	7.7587	7.8356	7.8688	7.96762	7.92626	7.9470
A <sub>3</sub> (cm <sup>2</sup> )	13–16	0.645	0.645	0.645	0.64502	0.645	0.6450
A <sub>4</sub> (cm <sup>2</sup> )	17–18	0.645	0.645	0.645	0.645	0.645	0.6450
A <sub>5</sub> (cm <sup>2</sup> )	19–22	9.0202	8.1183	8.1626	8.15323	8.01428	8.2415
A <sub>6</sub> (cm <sup>2</sup> )	23–30	8.2567	8.1338	7.9502	7.96666	7.96025	7.9290
A <sub>7</sub> (cm <sup>2</sup> )	31–34	0.645	0.645	0.6452	0.645	0.645	0.6450
A <sub>8</sub> (cm <sup>2</sup> )	35–36	0.645	0.645	0.645	0.645	0.645	0.6619
A <sub>9</sub> (cm <sup>2</sup> )	37–40	12.045	12.6231	12.2668	12.92718	12.79033	13.3314
A <sub>10</sub> (cm <sup>2</sup> )	41–48	8.0401	8.0971	8.1845	8.12258	8.1013	8.0185
A <sub>11</sub> (cm <sup>2</sup> )	49–52	0.645	0.645	0.6451	0.64518	0.645	0.6450
A <sub>12</sub> (cm <sup>2</sup> )	53–54	0.645	0.645	0.6451	0.645	0.64734	0.6450
A <sub>13</sub> (cm <sup>2</sup> )	55–58	17.38	17.3908	17.9632	17.05237	17.46153	16.5843
A <sub>14</sub> (cm <sup>2</sup> )	59–66	8.0561	8.0634	8.1292	8.06175	8.13039	8.0076
A <sub>15</sub> (cm <sup>2</sup> )	67–70	0.645	0.645	0.645	0.645	0.645	0.6451
A <sub>16</sub> (cm <sup>2</sup> )	71–72	0.645	0.645	0.645	0.645	0.64505	0.6450
Weight (kg)	327.691	327.653	327.77	327.568	327.575	327.691	325.871
Mean (kg)	329.89	327.76	327.99	328.684	327.693	329.89	333.059
SD (kg)	2.59	0.06	0.19	0.73	0.125	2.59	9.63
$f_1$	-	4.0000	4.0000	4.0000	4.0000	4.0000	3.9990
$f_3$	-	6.0000	6.0000	6.0000	6.0000	6.0000	5.9999
Constraint 1	-	NA	NA	NA	NA	NA	-2.09E-13
Constraint 2	-	NA	NA	NA	NA	NA	3.29E-14

efficiency of the ISA. The sensitivity of truss optimization problems to various BCH approaches was also investigated for the first time in the literature. This study clearly demonstrated the impact of BCH methods on the optimized design of truss structures. Methods such as PEBCH, Conservation, EBCH and Absorbing provided consistently better results than other BCH methods. Moreover, the results confirmed that the best value of  $\theta$  ranges between 0.75 and 3, and the optimum weight changes marginally if  $\theta$  remains within this domain.

The benchmark design examples in this study included both 2-D and 3-D truss structures. In order to further verify the performance of the ISA on more complex structures, our future work will involve the application of the ISA on large-scale 2-D truss structures, such as the planar 200-bar truss<sup>46</sup> and spatial 942-bar tower, as well as the spatial 224-bar truss.<sup>47,48</sup> Investigation into automatic tuning of the parameter depending on the problem context can be another research topic.

## ACKNOWLEDGMENTS

The authors would like to thank the editor and reviewers for their comments and suggestions. The authors would also like to acknowledge Farhad Zeighami for his work on the initial version of this paper.

## PEER REVIEW INFORMATION

*Engineering Reports* thanks the anonymous reviewers for their contribution to the peer review of this work.

## CONFLICT OF INTEREST

The authors declare no potential conflict of interest.

## AUTHOR CONTRIBUTIONS

**Ali Kashani:** Formal analysis; investigation; methodology; writing-original draft. **Raymond Chiong:** Conceptualization; methodology; supervision; writing-review & editing. **Sandeep Dhakal:** Investigation; writing-review & editing. **Amir Gandomi:** Conceptualization; methodology; supervision.

## DATA AVAILABILITY STATEMENT

The data generated in this study are available from the first author (A.R.K.— kashani.alireza@ymail.com ) upon request.

## ORCID

Ali R. Kashani  <http://orcid.org/0000-0002-0950-8789>

Raymond Chiong  <https://orcid.org/0000-0002-8285-1903>

## REFERENCES

1. Gandomi AH, Kashani AR, Roke DA, Mousavi M. Optimization of retaining wall design using evolutionary algorithms. *Struct Multidiscip Optim.* 2017;55(3):809-825.
2. Gandomi AH, Kashani AR, Roke DA, Mousavi M. Optimization of retaining wall design using recent swarm intelligence techniques. *Eng Struct.* 2015;103:72-84.
3. Gandomi AH, Kashani AR. Automating pseudo-static analysis of concrete cantilever retaining wall using evolutionary algorithms. *Measurement.* 2018;115:104-124.
4. Kashani AR, Gandomi M, Camp CV, Gandomi AH. Optimum design of shallow foundation using evolutionary algorithms. *Soft Comput.* 2020;24(9):6809-6833.
5. Gandomi AH, Kashani AR. Construction cost minimization of shallow foundation using recent swarm intelligence techniques. *IEEE Trans Ind Inform.* 2017;14(3):1099-1106.
6. Camp CV, Huq F. CO 2 and cost optimization of reinforced concrete frames using a big bang-big crunch algorithm. *Eng Struct.* 2013;48:363-372.
7. Hasançebi O, Kazemzadeh Azad S. Discrete size optimization of steel trusses using a refined big bang-big crunch algorithm. *Eng Optim.* 2014;46(1):61-83.
8. Gandomi AH, Yang XS, Talatahari S, Alavi AH. Metaheuristic algorithms in modeling and optimization. In: Gandomi AH, Yang X-S, Talatahari S, Alavi AH, eds. *Metaheuristic Applications in Structures and Infrastructures*. Oxford, UK: Elsevier; 2013:1-24.
9. Gandomi AH, Kashani AR, Mousavi M, Jalalvandi M. Slope stability analyzing using recent swarm intelligence techniques. *Int J Numer Anal Methods Geomech.* 2015;39(3):295-309.
10. Gandomi AH, Kashani AR, Mousavi M, Jalalvandi M. Slope stability analysis using evolutionary optimization techniques. *Int J Numer Anal Methods Geomech.* 2017;41(2):251-264.
11. Sahab MG, Toropov VV, Gandomi AH. Traditional and modern structural optimization techniques – theory and application. In: Gandomi AH, ed. *Metaheuristic Applications in Structures and Infrastructures*. Oxford, UK: Elsevier; 2013:25-47.



12. Yang XS, Bekdaş G, Nigdeli SM, eds. *Metaheuristics and Optimization in Civil Engineering*. Vol 7. New York, NY: Springer; 2015.
13. Kashani AR, Gandomi AH, Mousavi M. Imperialistic competitive algorithm: a metaheuristic algorithm for locating the critical slip surface in 2-dimensional soil slopes. *Geosci Front*. 2016;7(1):83-89.
14. Gandomi AH, Kashani AR, Mousavi M. Boundary constraint handling affection on slope stability analysis. *Engineering and Applied Sciences Optimization*. Switzerland: Springer International Publishing; 2015:341-358.
15. Gandomi AH, Kashani AR, Zeighami F. Retaining wall optimization using interior search algorithm with different bound constraint handling. *Int J Numer Anal Methods Geomech*. 2017;41(11):1304-1331.
16. Gandomi AH, Kashani AR. Evolutionary bound constraint handling for particle swarm optimization. *Proceedings of the 4th International Symposium on Computational and Business Intelligence (ISCBI 2016)*; 2016; Olten, Switzerland.
17. Trivedi IN, Gandomi AH, Jangir P, Jangir M. Study of different boundary constraint handling schemes in interior search algorithm. In: Dash S, Vijayakumar K, Panigrahi B, Das S, eds. *Artificial Intelligence and Evolutionary Computations in Engineering Systems, Advances in Intelligent Systems and Computing*. Vol 517. Singapore: Springer; 2017:547-564.
18. Helwig S, Branke J, Mostaghim S. Experimental analysis of bound handling techniques in particle swarm optimization. *IEEE Trans Evol Comput*. 2013;17(2):259-271.
19. Padhye N, Mittal P, Deb K. Feasibility preserving constraint-handling strategies for real parameter evolutionary optimization. *Comput Optim Appl*. 2015;62(3):851-890.
20. Gandomi AH. Interior search algorithm (ISA): a novel approach for global optimization. *ISA Trans*. 2014;53(4):1168-1183.
21. Blum, C., Chiong, R., Clerc, M., De Jong, K., Michalewicz, Z., Neri, F., Weise, T. (2012). Evolutionary optimization. In Chiong R, Weise T, Michalewicz Z, *Variants of Evolutionary Algorithms for Real-World Applications* (pp. 1–29). Berlin Heidelberg: Springer.
22. Kashani AR, Chiong R, Mirjalili S, Gandomi AH. Particle swarm optimization variants for solving geotechnical problems: review and comparative analysis. *Arch Comput Methods Eng*. 2021;28:1871–1927.
23. Kaveh A, Ghazaan MI. A comparative study of CBO and ECBO for optimal design of skeletal structures. *Comput Struct*. 2015;153:137-147.
24. Coello CAC, Carlos A. A survey of constraint handling techniques used with evolutionary algorithms. Lania-RI-99-04; 1999; Laboratorio Nacional de Informática Avanzada.
25. Becerra RL, CoelloCoello CA. Cultured differential evolution for constrained optimization. *Comput Methods Appl Mech Eng*. 2006;195:4303-4322.
26. Cheng S, Shi Y. Diversity control in particle swarm optimization. *Proceedings of the 2011 IEEE Symposium on Swarm Intelligence*; 2011:1–9.
27. Gandomi AH, Yang XS. Evolutionary boundary constraint handling scheme. *Neural Comput Appl*. 2012;21:1449-1462.
28. Arabas J, Szczepankiewicz A, Wroniak T. Experimental comparison of methods to handle boundary constraints in differential evolution. In: Schaefer R, Cotta C, Kołodziej J, Rudolph G, eds. *Parallel Problem Solving from Nature, PPSN XI, Series Lecture Notes in Computer Science*. Vol 6239. Berlin Heidelberg: Springer; 2010:411-420.
29. Bratton D, Kennedy J. Defining a standard for particle swarm optimization. *Proceedings of the IEEE Swarm Intelligence Symposium*; 2007:120-127.
30. Zhang WJ, Xie XF, Bi DC. Handling boundary constraints for numerical optimization by particle swarm flying in periodic search space. *Proceedings of the IEEE Congress on Evolutionary Computation (CEC 2004)*; 2004:2307-2311.
31. Alvarez-Benitez JE, Everson RM, Fieldsend JE. A MOPSO algorithm based exclusively on pareto dominance concepts. *Proceedings of the International Conference on Evolutionary Multi-Criterion Optimization*; 2005:459-473.
32. Gandomi AH, Kashani AR. Probabilistic evolutionary bound constraint handling for particle swarm optimization. *Oper Res*. 2018;18(3):801-823.
33. He S, Prempain E, Wu QH. An improved particle swarm optimizer for mechanical design optimization problems. *Eng Optim*. 2004;36(5):585-605.
34. Sedaghati R, Suleman A, Tabarrok B. Structural optimization with frequency constraints using the finite element force method. *AIAA J*. 2002;40(2):382-388.
35. Kaveh A, Zolghadr A. Democratic PSO for truss layout and size optimization with frequency constraints. *Comput Struct*. 2014;130:10-21.
36. Kaveh A, Javadi SM. Shape and size optimization of trusses with multiple frequency constraints using harmony search and ray optimizer for enhancing the particle swarm optimization algorithm. *Acta Mech*. 2014;225(6):1595-1605.
37. Gomes HM. Truss optimization with dynamic constraints using a particle swarm algorithm. *Expert Syst Appl*. 2011;38(1):957-968.
38. Miguel LFF, Miguel LFF. Shape and size optimization of truss structures considering dynamic constraints through modern metaheuristic algorithms. *Expert Syst Appl*. 2012;39(10):9458-9467.
39. Khatibinia M, Naseralavi SS. Truss optimization on shape and sizing with frequency constraints based on orthogonal multi-gravitational search algorithm. *J Sound Vib*. 2014;333(24):6349-6369.
40. Farshchin M, Camp CV, Maniat M. Multi-class teaching-learning-based optimization for truss design with frequency constraints. *Eng Struct*. 2016;106:355-369.
41. Wang D, Zhang WH, Jiang JS. Truss optimization on shape and sizing with frequency constraints. *AIAA J*. 2004;42(3):622-630.
42. Wei L, Tang T, Xie X, Shen W. Truss optimization on shape and sizing with frequency constraints based on parallel genetic algorithm. *Struct Multidiscip Optim*. 2011;43(5):665-682.
43. Lin JH, Che WY, Yu YS. Structural optimization on geometrical configuration and element sizing with statical and dynamical constraints. *Comput Struct*. 1982;15(5):507-515.
44. Kaveh A, Ghazaan MI. Enhanced colliding bodies algorithm for truss optimization with frequency constraints. *J Comput Civ Eng*. 2015;29(6):04014104.

45. Kaveh A, Ghazaan MI. Hybridized optimization algorithms for design of trusses with multiple natural frequency constraints. *Adv Eng Softw.* 2015;79:137-147.
46. Tejani GG, Savsani VJ, Patel VK. Adaptive symbiotic organisms search (SOS) algorithm for structural design optimization. *J Comput Des Eng.* 2016;3(3):226-249.
47. Kaveh A, Talatahari S. Size optimization of space trusses using big bang–big crunch algorithm. *Comput Struct.* 2009;87(17–18):1129-1140.
48. Hasancebi O, Erbatur F. Layout optimization of trusses using improved GA methodologies. *Acta Mech.* 2001;146(1–2):87-107.

**How to cite this article:** Kashani AR, Chiong R, Dhakal S, Gandomi AH. Investigating bound handling schemes and parameter settings for the interior search algorithm to solve truss problems. *Engineering Reports.* 2021;3:e12405. <https://doi.org/10.1002/eng2.12405>